Bulletin of the Mineral Research and Exploration

http://bulletin.mta.gov.tr

Neotectonics and geothermal potential of the East Anatolian Tectonic Block: A case study in Diyadin (Ağrı) geothermal field, NE Türkiye

Ali KOÇYİĞİT[a]

[a]*Middle East Technical University, Department of Geological Engineering, Active Tectonics and Earthquake Research Lab, Ankara, Turkiye*

Research Article

Keywords:
Diyadin Geothermal Field, Thermogene Fissure-ridge Travertine, Active Volcano, Active Strike-slip Tectonic Regime.

ABSTRACT

Diyadin is situated 71 km ESE of Ağrı nearby the Turkish-Iranian State border in the east Anatolian tectonic block. It is only one of several type localities of promising geothermal fields in eastern Anatolia. The neotectonic regime and related fault zones in the eastern Anatolia are dominated by a strike-slip tectonic regime governed by a stress field state, in which the greatest principal compressive stress (σ1) is operating in NNW direction (N22°W) while the least principal stress axis (σ3) or extension direction is N68°E. This stress field state was proved once more by the tensor solution of the 12 June 2022 Akçift (Muradiye-Van) earthquake of Mw = 5.1. The strike-slip neotectonic regime started at the time of latest Pliocene-early Quaternary and then triggered the first occurrence of the fissure eruption along the NW trending Kaletepe open fracture. This event was followed by the development of both the two-peaked Tendürek strato-shild volcano and the Diyadin geothermal field (DGF). The most common manifestations of the DGF are the active tectonic regime and related faults, active volcanoes, fumeroles, numerous hot water springs to artesian wells, widespread iron-rich alteration zones, actively growing fissure-ridge travertines and the probable presence of the shallow-seated and unroofed hypabyssal felsic to intermediate intrusions of Quaternary age.

Received Date: 17.06.2022
Accepted Date: 07.02.2023

1. Introduction

In general, major factors, which control development of the geothermal fields, are active tectonic regime and related faults, plate boundaries and/or proximity to them, shallow-seated Curie point depth (CPD), high heat flow, young volcanic activity, young hypabyssal intrusions with felsic to intermediate chemical compositions, thinned crust and ascended asthenospheric mantle, a thick package of rocks with high porosity or reservoir rock (s), a package of impermeable rocks or cover rocks, and meteoric water supply enough. These factors also determine the distribution pattern of geothermal fields throughout the territory of Türkiye. For this reason, the most of geothermal fields (approximately 78%) are situated in the southwest Anatolia, i.e., at the back-arc region of the South Aegean-Cyprus subduction zone. In the same way, remainings are located within and adjacent to the active fault systems or plate boundaries such as the North Anatolian dextral strike-slip fault system, East Anatolian sisnistral strike-slip fault system and significant numbers of intraplate fault zones or systems such as the İnönü-Eskişehir, Akşehir-Afyon, and Central Anatolian active fault systems. The third and forth significant localities of the geothermal field are the central and eastern Anatolia respectively. They are characterized by the Quaternary volcanic activities (Innocenti et al., 1976; Ercan et al., 1993). According to Akın et al. (2014), the areas in which the heat flow

Citation Info: Koçyiğit, A. 2023. Neotectonics and geothermal potential of the East Anatolian Tectonic Block: A case study in Diyadin (Ağrı) geothermal field, NE Türkiye. Bulletin of the Mineral Research and Exploration 171, 33-68. https://doi.org/10.19111/bulletinofmre.1248712

**Corresponding author: Ali KOÇYİĞİT, alikocyigit45@gmail.com*

is between 0-125.7 mW/m^2 are called as normal fields, whereas the areas in which the heat flow is higher than 125.7 mW/m^2 are called as the geothermal fields. In addition, around Ağrı and its near environ in the eastern Anatolia, the average heat flow varies from 60 to 80 mW/m², i.e., it is low, and this area is not a geothermal field (Akın et al., 2014). Whereas, Aydın et al. (2020) reported that the eastern Anatolia is in the nature of low- or moderate-temperature geothermal systems based on some geological factors such as relatively thick crust, low surface heat flux and the absence of ideal cover units.

According to 2017 data, the energy consumption of Türkiye is provided by 31% from petrol, 28.2% from natural gas, 27.3% from coal and 12.5% from hydraulic and other renewable energy sources (Canbaz et al., 2020). The number of electricity energy production plants in the country reached 3098 by the end of July 2017. The country's energy needs are supplied by 288 natural gas, 186 wind, 613 hydraulic, 40 coal, 33 geothermal, 1.773 solar and 165 other power plants (MTA, 2018). The basic renewable energy sources are solar, wind, geothermal and hydroelectric. Theoretically, it is thought that the Türkiye's geothermal capacity is 31500 MWt, and its 77.9% is in the western Anatolia. The geothermal electricity potential is about 2000 MWe, whereas the installed capacity of electricity energy producted from geothermal resource is only 201.1 MWe at the end of 2017. The number of plants is 67 and its share in the primary energy balance is only 0.2% (Canbaz et al., 2020). Türkiye, there are 276 geothermal occurrences including nearly 110 fields with an average surface temperatures ranging from 22.5°C to 220°C (maximum 242°C). The surface temperatures in 80 of the occurrences are above 60°C, in 13 of them above 100°C and in 8 of ccurrences above 140°C (Basel et al., 2010). They have also reported that one of the major geothermal fields in the eastern Anatolia is the Diyadin (Ağrı) area where the average flow rate is 561 lt/s, the average surface temperature is 72°C, and the temperature interval at 1km depth is 55°-85°C.

In general, eastern Anatolia does not seem to present promising geothermal fields in spite of its extensive and young volcanism (Serpen et al., 2009). However, there are several well-known promising geothermal fields in the eastern Anatolia. These are the Nemrut Caldera, Başkale-Yiğit stratovolcano, Erciş-Zilan and the Tendürek volcano-Diyadin geothermal fields. The lack of good geothermal resources requires a geothermal-based multidisciplinary studies, i.e., there is a need for detailed hydrochemical, volcanological, tectonical and systematic geophysical investigations of the volcanic structures in the eastern Anatolia (Serpen et al., 2009). In the eastern Anatolia, geothermal-based detailed multi-disciplinary studies are very limited (Basel et al., 2010; Pasvanoğlu, 2013; Aydın et al., 2020; Şener and Şener, 2021). These studies are focusud to the geothermal potential of Ağrı region. Pasvanoğlu (2013) reported that the temperatures of the deep geothermal reservoirs in Diyadin range between 92° and 156°C based on quartz geothermometry. Same author has also stated that Diyadin waters are heated by magmatic activity associated with the Tendurek volcano based on chemical data. Şener and Şener (2021) reported that, the Ağrı provincial center, Patnos, Eleşkirt, and Doğubayazıt regions have high geothermal potential, while the Diyadin area has been identified as a very high geothermal potential based on the the Geothermal Potential Index (GPI) map of the Ağrı area (MTA, 2021).

Our study aims to present active tectonics, major surface manifestations, such as the fissure-ridge travertines, fumaroles and wide-spread alteration zones, of the Diyadin geothermal field, and the conceptual geothermal model for the eastern Anatolia under the lights of both the natural to international literature and detailed field geological data newly obtained from the field geological mapping studies carried out in Diyadin and its near environ. Thus, we think to fill the gap in the national and international geothermal literatures, and to increase the share of the renewable energy in the balance of primary energy used in our country.

2. Regional Geological Setting

The study area is situated very close to the Turkish-Iranian State border in the East Anatolian Tectonic Block (EATB). The EATB or the northwestern section of the Anatolian-Iranian high plateau (up to average 2 km above the sea level) is bounded by the Lesser Caucasus fold-thrust belt to the northeast, by the Kelkit-Çoruh sinistral strike-slip fault zone to the northwest, by both the North Anatolian and East Anatolian Fault systems to the west, by the Bitlis-Zagros Suture Zone (BZSZ) to the south and by the Turkish-Iranian State

border to the east (Figure 1). The eastern Anatolia is a seismically very active and geologically complicated region included in the Arabian-Eurasian collision zone (Figure 1a). The geological complexity is characterized by fold-thrust fault belts, strike-slip faults and related basin formations. These characteristics of the eastern territory of Türkiye represent a natural laboratory to observe multi-stage deformation. The geologically complicated multi-stage deformation pattern has been formed by the entirely demise of the Tethyan Seaway, the Bitlis Ocean, between the Indian Ocean and the east Mediterranean Sea followed by the continent-continent collision of northerly moving Arabian Plate and the Eurasian plate during the late Serravalian time (Şengör and Yılmaz, 1981; Dewey et al., 1986). These authors accepted that the late Serravalian time is the onset age of the neotectonic regime in Türkiye. However, after the final collision and formation of the Bitlis suture zone, the N-S-directed intracontinental convergence lasted over a time period of ~9 Ma. This time slice of ~9 Ma is here termed as the transitional period between the contractional palaeotectonic and the strike-slip neotectonic regimes (Koçyiğit et al., 2001; Aksoy et al., 2007; Çolak et al., 2012; Koçyiğit, 2013; Koçyiğit and Canoğlu, 2017). During this transitional period, a series of deformations took place. Some of them are the thickening of crust, regional tectonic uplift, E-W trending folds, thrust to reverse faults, resetting of new drainage system, disappearance of marine conditions, development of short-to long-term stratigraphic gaps and a widespread post-collisional volcanic activitity (Şengör and Kidd, 1979; Innocenti et al., 1980; Dewey et al., 1986; Şaroğlu and Yılmaz, 1986; Yılmaz et al., 1987; Ercan et al., 1990; Koçyiğit and Beyhan 1998; Koçyiğit et al., 2001; Koçyiğit, 2013; Koçyiğit and Canoğlu, 2017). The contractional deformation and development of fold-thrust belts lasted until the late Pliocene, and then they were replaced by a new tectonic regime, namely the contractional-extensional regime, i.e., the prominent strike-slip faulting-related tectonic regime. This is proved by the occurrence of a series of inversions. These are the inversions in the deformational style, types of geological structures, the nature of sedimentation and basin formation, geochemical characteristics of the volcanic activity (e.g., changing from calc-alkali nature to dominantly alkali composition), the nature of seismic activity triggered by the formation of two intracontinental transform fault boundaries (North Anatolian dextral strike-slip and the East Anatolian sinistral strike-slip fault systems), and finally west-southwestward escapement of the Anatolian platelet along these two megashears (Hempton, 1987; Koçyiğit and Beyhan 1998; Koçyiğit et al., 2001; Koçyiğit, 2013; Koçyiğit and Canoğlu, 2017). Hence the onset age of the strike-slip dominated neotectonic regime in eastern Anatolia is the late Pliocene (Koçyiğit et al., 2001; Koçyiğit, 2013; Koçyiğit and Canoğlu, 2017). In this neotectonic regime the greatest principal stress axis ($\sigma 1$) is operating in approximately NNW direction. In addition to the compression orientation, one other NE-SW secondary orientation is also observed which has been prevailing in the northeastern section of the EATB since the beginning of Quaternary period (Jackson, 1992; Copley and Jackson, 2006; Mokhoori et al., 2021). On a regional scale the principal stress axes orientations, which govern the strike-slip neotectonic regime in eastern Anatolia, are mainly controlled by the Arabian-Eurasian plate convergence. However, local stress orientations have been significantly influenced from the secondary blocks motions and their geometries (Avagyan et al., 2005). Based on the current stress field state, two major groups of strike-slip faulting-related structures occur in the EATB and its near environ. These are: (1) NE trending sinistral strike-slip faults, and (2) NW trending dextral strike-slip faults. From northwest to southeast the Kelkit-Çoruh, Erzurum, Dumlu, Çobandede, Digor and Başkale fault zones comprise the first group of active structures (Arpat et al., 1977; Şaroğlu and Yılmaz, 1986; Şaroğlu et al., 1987; Koçyiğit et al., 2001; Emre et al., 2012; Koçyiğit, 2013; Koçyiğit and Canoğlu, 2017; Emre et al., 2018). In contrast to this group, from northeast to southwest, the Aras, Iğdır, Balıkgölü, Ağrı, Çaldıran, North Tebriz, Karayazı, Erciş-Dorutay and the Yüksekova fault zones form the second group of active structures (Koçyiğit et al., 2001; Hessami et al., 2003; Karakhanian et al., 2004; Masson et al., 2006; Copley and Jackson, 2006; Dhont and Chorovicz, 2006; Djamour et al., 2011; Shabanian et al., 2012; Koçyiğit, 2013; Sharkov et al., 2014; Sağlam and Selçuk et al., 2016; Aghajany et al., 2017; Emre et al., 2018; Güneyli et al., 2020; Sağlam-Selçuk and Kul, 2021; Mokhoori et al., 2021). In addition to these structures, there are also a series of ~ N-S trending oblique-slip normal faults, and approximately E-W trending thrust to reverse faults, one of which reactivated and caused to the occurrence of a very destructive earthquake, the 23 October 2011 Tabanlı (Van) earthquake of Mw=7.2 (Koçyiğit, 2013). The most of these structures are outside of the present study. However, the Iğdır, Aras, Balıkgölü, Ağrı, Çaldıran, Erciş-Dorutay and the North Tebriz

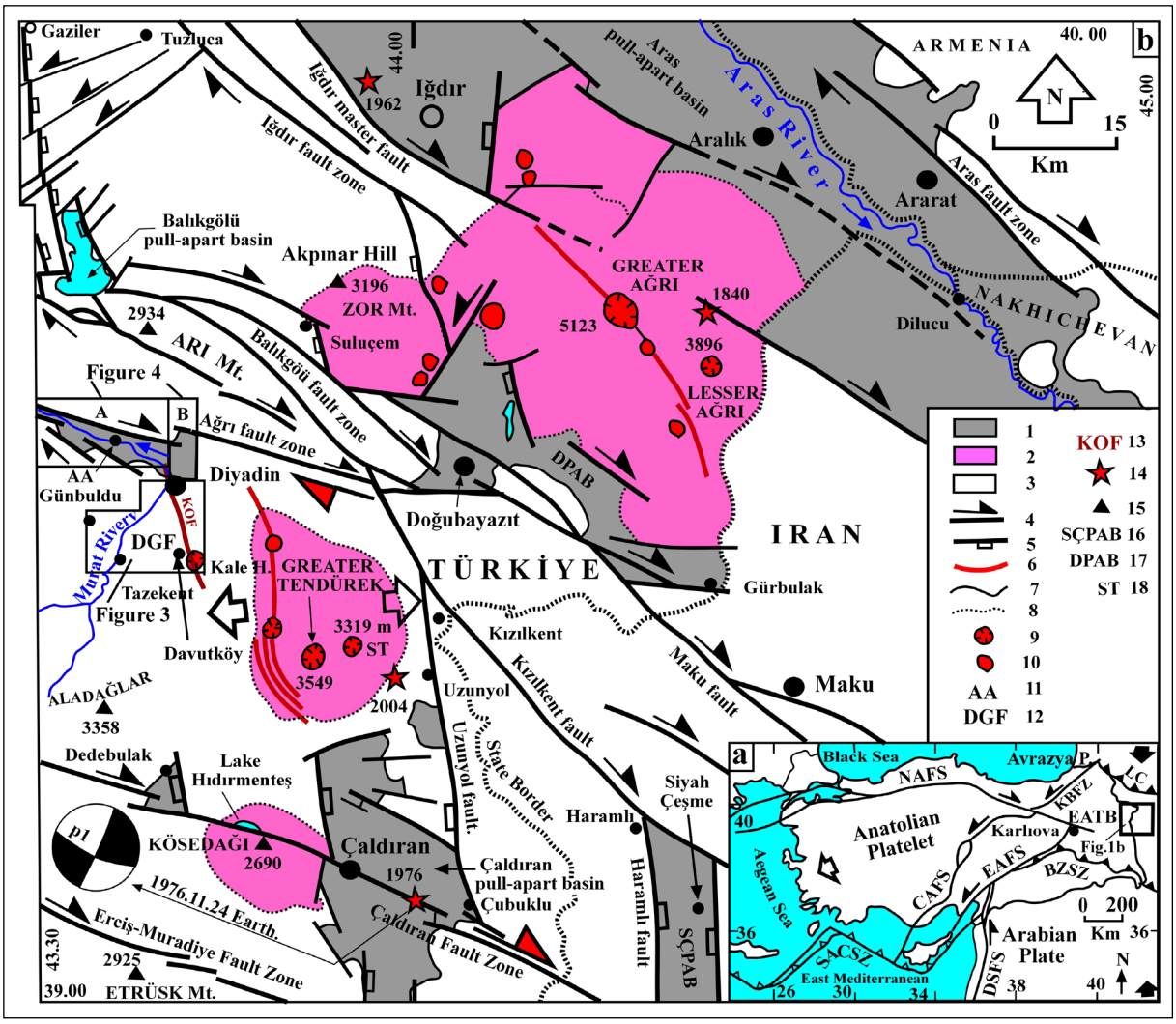

Figure 1- a) Simplified tectonic map illustrating significant neotectonic strucures in Türkiye and adjacent areas, and location of the study area. BZSZ: Bitlis-Zagros Suture Zone, EAFZ: East Anatolian Fault System, EATB: East Anatolian Tectonic Block, NAFS: North Anatolian Fault System, KBFZ: Kelkit-Bayburt Fault Zone, LC: Lesser Caucasus Fold-Thrust Belt, CAFS: Central Anatolian Fault System, DSFS: Dead Sea Fault System, b) Simplified regional neotectonic map of the study area and near environ. AA: Aşağıakpazar, DGF: Diyadin geothermal field, KOF: Kaletepe open fracture; 1. Quaternary pull-apart basin fill, 2. Quaternary volcanic cones, 3. Pre-Quaternary rocks, 4. Strike-slip faults, 5. Normal faults, 6. Open fractures, 7. Formation boundary, 8. Possible boundary, 9. Crater, 10. Other eruption centers, 11. Aşağı Akpazar, 12. Diyadin geothermal area, 13. Kaletepe open fracture, 14. Earthquakes epicenters, 15. Elevation above sea level; Large closed arrows indicate regional contraction directions, while large open arrows indicate regional extension directions (Note: contracion and extension are still going on).

fault zones are the key structures taking a part in the development of the Diyadin geothermal field (DGF). For this reason, they are described in detail in the following sections.

3. Stratigraphical Outline of Diyadin Geothermal Field (DGF)

The study area is the Diyadin geothermal field (DGF). It is situated at approximately 71 km east of the city of Ağrı along the Ağrı-Doğubeyazıt-Iran highway. It covers an area of approximately 100 km² surrounded by the Diyadin county, Davutköy, Tazekent, Dibekli, Altınkilit, Günbuldu and Aşağıakpazar villages respectively (Figure 1b). The development of the DGF is still lasting at the northwest foot of the polygenetic and double-peaked Tendürek volcano of late Quaternary age located at the upstream side of the 722 km long antecedent Murat River system (Figure 1b). The diagnostic characteristics of the DGF are

the occurrences of numerous hot water springs and actively growing fissure-ridge travertines in different directions. The reservoir is one of the key factors in the development of the geothermal field. For this reason, not only the younger neotectonic rock units, but also the older paleotectonic rock units are described here.

Based on ages, deformation pattern and the types of tectonic regimes, which controlled both the deposition and the deformation pattern of rocks, the rocks units exposing in and adjacent to the DGF are classified into two major categories: (1) paleotectonic units and (2) neotectonic units (Figure 2). The paleotectonic units,

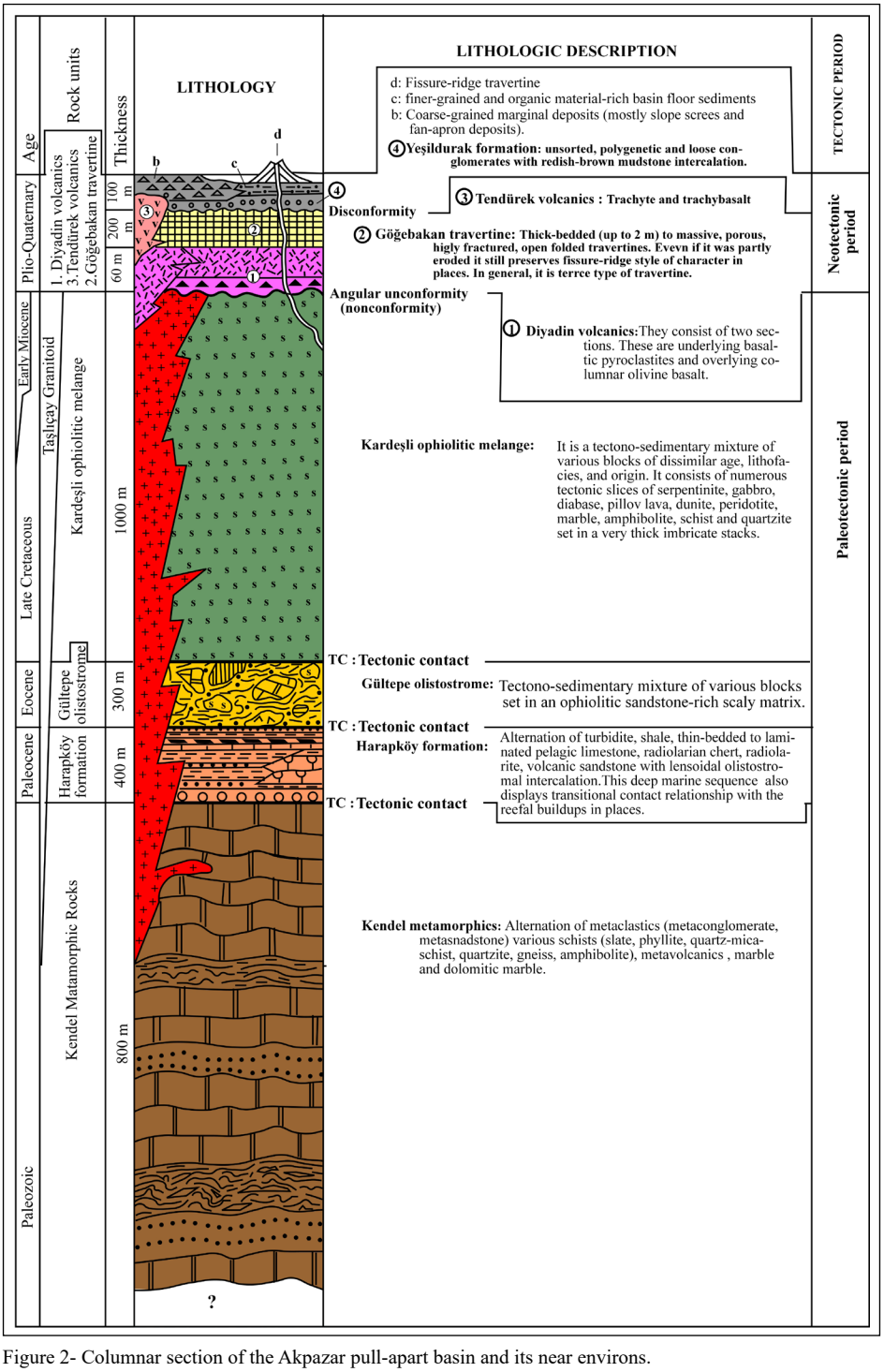

Figure 2- Columnar section of the Akpazar pull-apart basin and its near environs.

from oldest to youngest, are the Kendel Metemorphic Rocks, the Kardeşli ophiolitic mélange, the Harapköy formation, the Gültepe olistostrome, the Taşlıçay granitoid, the Dalören volcanic rocks, and the Mutlu formation. The neotectonic units are the Diyadin volcanic rocks, the Göğebakan travertines, the Yeşildurak fluvial sedimentary sequence, the Tendürek volkanic rocks, the Diyadin fissure-ridge travertines and the Quaternary alluvial sediments (Figures 3 and 4). Both the paleotectonic and neotectonic rock units are described separately below.

3.1. Paleotectonic Units

3.1.1. Kendel Metamorphic Rocks

This rock unit is exposed widely at the southwestern corner of the Akpazar pull-apart basin (Figure 4), near east of Günbuldu village and on the southwestern side of the Ulukent Town (Figure 3). Bottom of the Kendel metamorphic rocks is not exposed in the study area. However, at the visible lower section, the unit begins with the medium to thick bedded (30 cm-1.5 m),

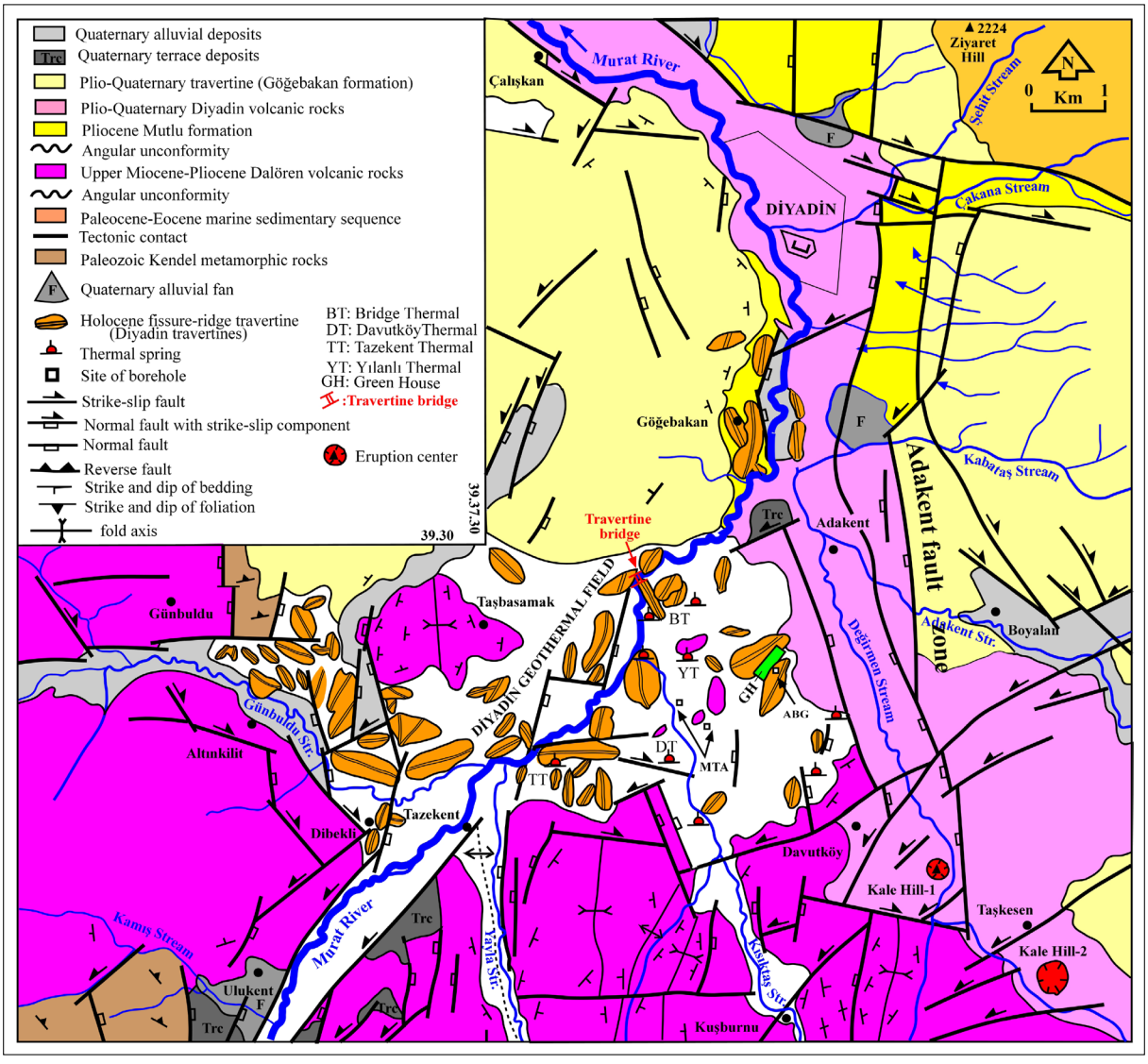

Figure 3- Geological map of the Diyadin geothermal field and its near environs.

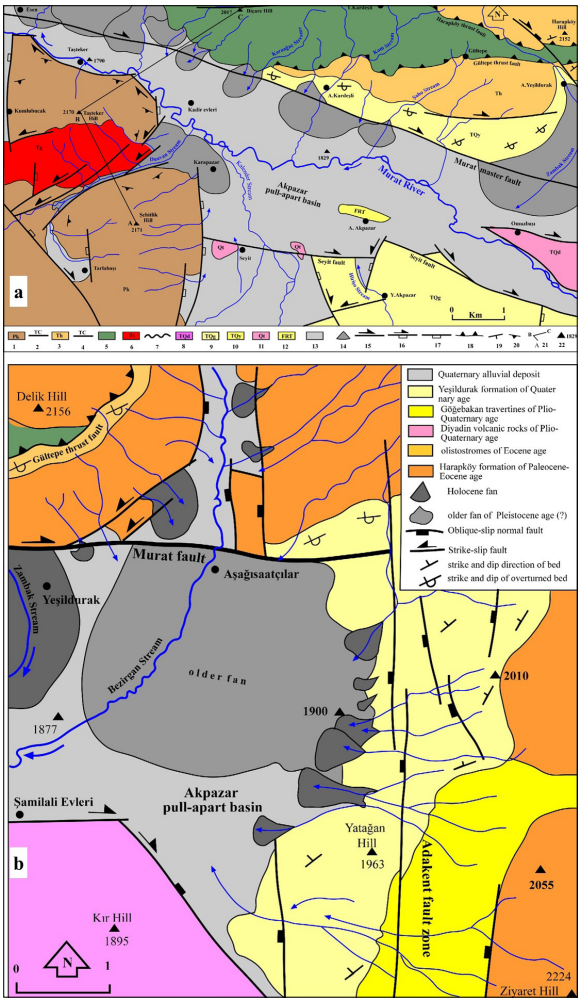

Figure 4- a) Geological map of the Akpazar pull-apart basin. 1- Paleozoic Kendel metamorphic rocks, 2- Tectonic contact, 3-Paleocene-Eocene marine sedimentary sequence, 4-Tectonic contact, 5-Upper Cretaceous ophiolitic melange, 6- Lower Miocene Taşlıçay Granitoid, 7- Angular unconformity (nonconformity), 8-Plio-Quaternary Diyadin columnar basalt, 9- Plio-Quaternary older travertine, 10- Plio-Quaternary fluvial conglomerate, 11- Quaternary Tendürek volcanics, 12- Quaternary alluvial sediments (basin fill), 13- Upper Quaternary fissure-ridge travertine, 14- alluvial fan, 15- Strike-slip fault, 16- Normal fault with strike-slip component, 17- Normal fault, 18- Thrust fault, 19- Strike and dip of bedding, 20- Strike and dip of foliation, 21- Line of geological cross-section, and 22- Elevations above sea level, b) Geological map of the eastern tip of the Akpazar pull-apart basin and its near environ.

in places massive, gray, blue and yellow colored dolomitic marbles, and then continues upwards with the alternation of marble, dolomitic marble, calcschist, mica-quartzschist, quartzite, amphibolite, gneiss and metaclastic rocks (metasandstone, metaconglomerate). At the topmost it ends with a thick package of recrystallized limestone. The visible total thickness of the Kendel metamorphic rocks is about 800 m. It is intruded and cut across by the Taşlıçay granitoid of the early Miocene age. However, it displays frequently faulted-contact relationships with younger rock units (Figures 3 and 4). The Kendel metamorphic rocks are also crossed frequently by the open fractures, shear planes and quartz veins owing to multiple deformation they have experienced. In addition, these rocks are full of caves of all size. For this reason, the Kendel metamorphic rocks, in particular marbels and quatrzites, are very porous and form main reservior of the geothermal fluid in the DGF. Based on previous works, age of the unit is Paleozoic (Esirtgen and Hepşen, 2018; Kansun et al., 2020).

3.1.2. Kardeşli Ophiolitic Mélange

This unit was previously reported as the "Kağızman Complex" by Kıral and Çağlayan (1980). It is exposed well in a large imbricate stack along the northern margin of the Akpazar pull-apart basin (Figure 4). The Kardeşli ophiolitic mélange displays tectonic contact relationships with the deep marine pelagic sedimentary sequence and olistostromes of Paleocene-Eocene age (Figure 5), while it is overlain with an angular unconformity by the Quaternary fluvial sedimentary sequence of the Akpazar pull-apart basin (Figure 6). The Kardeşli ophiolitic mélange consists of two major rock assemblages mixed by the tectono-sedimentery processes in a turbiditic scaly matrix. These are the deep-marine oceanic sedimentary sequence of pelagic limestone and radiolarian chert, and the spilite, pillove lava, basalt, diabase, gabbro, serpentinite and peridotite of oceanic crust to upper mantle lithosphere origin. It also contains rarely various blocks of marbles, quartzite, schists and shallow-water recrystallized limestones of continental crust origin. Whole of these rock assemblages are intensely sheared, brecciated and thrown into a series of wedge like imbricates. They display a southward-facing overturned to recumbent fold-thrust fault structure. This kind of outcrop pattern, chaotic internal structure and the thrust-faulted imbricate structure altogether reveal an accretionary prism formed at the inner wall of an oceanic trench situated adjacent to the overriding continental plate. Consequently, the Kardeşli ophiolitic mélange was

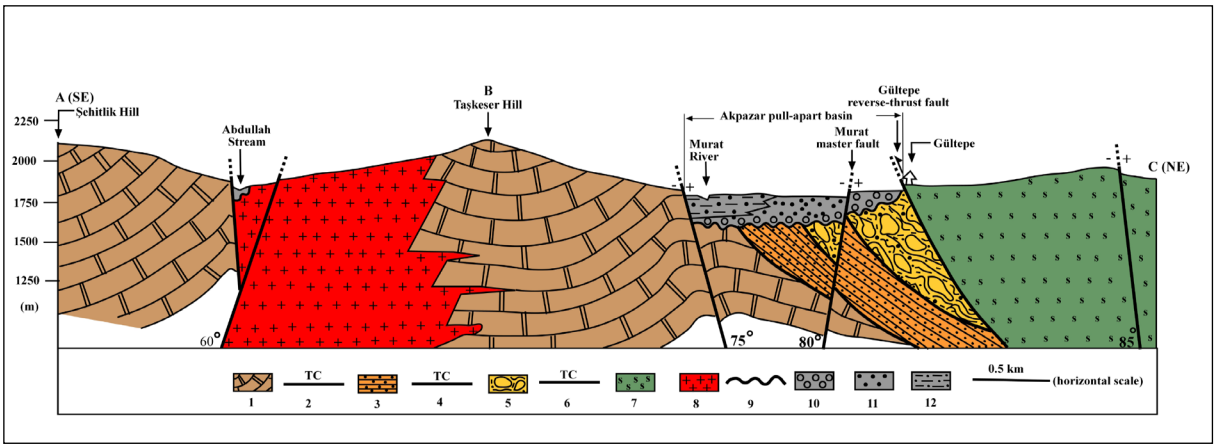

Figure 5- Geological cross-section along the line A-B-C on Figure 4; 1-Paleozoic Kendel metamorphic rocks, 2- Tectonic contact (TC), 3-Upper Paleocene Harapköy formation, 4- Tectonic contact (TC), 5-Eocene Gültepe olistostrome, 6- Tectonic contact (TC), 7-Upper Cretaceous Kardeşli ophiolitic melange, 8- Lower Miocene Taşlıçay Granitoid, 9-Angular unconformity (Nonconformity), 10-Plio-Quaternary polygenic fluvial conglomerate of the Yeşildurak formation, 11- Quaternary coarse-grained marginal deposits of basin, and 12- Finer grained depocentral deposits of the Akpazar pull-apart basin.

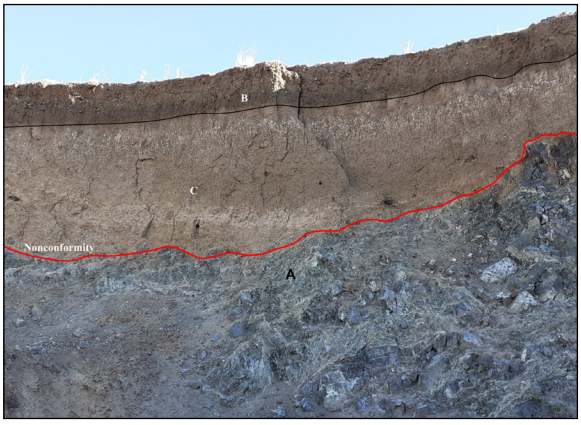

Figure 6- Close-up view of the nonconformity (angular unconformity) between the underlying serpentinite (A) of the Kardeşli ophiolitic mélange and the overlying fluvial sedimentary sequence (B) of the Yeşildurak formation, (C) Holocene soil horizon (near north of Yeşildurak village).

an originally accretionary prism or wedge resulted from sediments accreted onto the overriding tectonic plate along the convergent plate boundary. Most of the material in the accretionary wedge consists of marine sediments scraped off from the down-going slab of oceanic crust, but in some cases it also includes the erosional products of volcanic island arcs formed on the overriding plate.

The total thickness of the unit in the study area is 1 km. The deep sea pelagic limestones, mudstones and turbidites which comprise the matrix of the Kardeşli ophiolitic mélange. They contain rich foraminifers such as *Globotruncana stuarti, Globotruncana arca* and *Rugoglobigerina* sp (Aksoy and Tatar, 1990). Based on this fossil content, a Campanian-Maastrichtian age is assigned to the tectono-sedimentary mixture of the Kardeşli ophiolitic mélange. This unit is also reported widely as the East Anatolian Accretionary Prism (EAAP) in both native and international literature (Şengör and Yılmaz, 1981). The Kardeşli ophiolitic mélange, in particularly the mega-marble and carbonate blocks in it, represent the reservoir of the geothermal fluids in DGF.

3.1.3. Harapköy Formation and Gültepe Olistostrome

These rocks were previously named and reported as the "Pekiydere" and "Dirbi" formations, respectively, by Ercan and Sümengen (2018). In contrast to them, in the present study, they were renamed due to their different stratigraphical position in the study area (Figures 2 and 4). Both the Harapköy formation and the Gültepe olistostrome are exposed well around Ziyaret Hill to the near NE of Diyadin, and in the area among Aşağı Kardeşli, Gültepe, Aşağı Yeşildurak and Aşağısaatçılar villages and mostly on the Harapköy to Delik Hills along the northestern margin and eastern margins of the Akpazar pull-apart basin (Figures 3, 4a and 4b). At some localities, they were not mapped separately, because the Gültepe olistostrome also occurs as the intercalations within the Harapköy formation. Indeed, the Kardeşli ophiolitic mélange,

the Harapköy formation and the Gültepe olistostrome altogether form a thick imbricate stack separated by the intervening imbricate thrust faults (Figure 6). The Harapköy formation is composed of thin bedded to laminated deep marine shale, turbidite, palagic limestone, radiolarite and radiolarian chert alternation with polygenetic and unsorted olistostrome intercalations. This sedimentary succsession is intensely deformed (tight to overturned in position and also recumbent folded in places, especially against the tectonic contact with the Kardeşli ophiolitic mélange. The Harapköy formation contains thick-bedded to massive reefal limestone blocks of dissimilar size derived nearby steeply sloping wall of trench. The total thickness of the Harapköy formation is approximately 400 m. Based on the rich foraminifers content of the pelagic limestones and radiolarite, a late Paleocene-early Eocene age was assigned to the Harapköy formation (Ercan and Sümengen, 2018). The Gültepe olistostrome is exposed as an imbricate slice between the overlying ophiolitic mélange and the underlying Harapköy formation (Figures 4 and 6). It is a tectono-sedimentary mixture of various angular to sub-rounded blocks of all sizes set in a ophiolitic material-rich turbiditic matrix. Among blocks marble, quartzite, schists, reefal limestone, radiolarian chert, pelagic limestone, diabase, spilit, serpentinite, peridotite, gabbro, and pillow basalt can be mentioned. Based on the stratigarphical position and types of blocks included in it, an Eocene age was assigned to the Gültepe olistostrome.

3.1.4. Taşlıçay Granitoid

This igneous rock is exposed along the southern slope of the Taşteker Hill along the western margin of the Akpazar pull-apart basin (Figure 4). In addition, it also exposes at several localites on the upstream side and Aladağlar drainage divide to the south and outside of the study area (Figure 1b). At this locality (Çukuryala) the granodiorite displays a transitional contact relationship with the rhyolites and related pyroclastites. This contact relationship and their chemical composition reveal that their origin is same, i.e., it is a hypabyssal falsic intrusion. In general, the Taşlıçay granitoid is gray to pinkish in colour, and it has been densely fractured and cut across frequently by small-scaled faults, shear planes and quartz veins. The Paleozoic Kendel metamorphic rocks have also been intruded and metamorphosed once more by the Taşlıçay granitoid in the study area (Figure 5). On a regional scale, i.e., in the East Anatolian collision zone, there are a number of felsic intrusion outcrops similar to the Taşlıçay granitoid. They have also cut across the different rock packages of the East Anatolian Accretionary Prism (EAAP) (Keskin, 2003; Açlan and Duruk, 2018). The Taşlıçay granitoid is one of them, and it consists of two different rock assemblages. These are the I-type (host rock is igneous) and S-type (host rock is sedimentary) intrusive igneous rock assemblages. The I-type intrusive igneous assamblage consists of gabbro, diorite, quartzdiorite and monzodiorit with mildly intermediate composition. In contrast to them, the S-type assemblage are composed of tonolite, granodiorite and granite with felsic composition. The Taşlıçay granitoids display enrichment in large ion lithophile elements (LILE) (Cs, Rb, Ba, U, Th, Pb), light rare earth element (LREE) (I-type; LaN/YbN = 7.38–17.53; S-type; LaN/YbN = 6.27–26.73), and depleted in high field strength element (HFSE) (Nb, Ta, P, Ti) implying a subduction-related magmatic signature (Açlan and Duruk, 2018). Consequently, the origin of the Taşlıçay granitoid must be a calc-alcaline hybrid magma. Both the final collision of the Arabian and Erasian plates and the entire demise of the intervening ocean floor occurred during the late Serravalian time (Şengör and Yılmaz, 1981; Dewey et al., 1986, Yılmaz et al., 1998). However, both the intra-continental convergence and the subduction have also lasted after the collision and led to the thickening of crust and uplift in the East Anatolia (Pearce et al., 1990; Yılmaz et al., 1998; Keskin 2003; Barazangi et al., 2006; Elitok and Dolmaz, 2014). Accordingly, the oceanic slab of the Arabian plate persisted to subdect deeper and deeper below the accretionary prism. For this reason, the ocenic slab was first steepened and then broke off which led to the partial melting of both the continental crust and the lithospheric mantle. Thus two kinds of magma (falsic and basic magmas) developed and they begun to rise. Finally, a hybrid magma formed by the mixing of these upwelling two magmas (Keskin, 2003; Açlan ve Duruk, 2018). The Taşlıçay granitoid might have been formed by the cooling and solidification of this hybrid magma at shallower depth. The young hypabissal felsic magma reservoirs preserve their temperature for a long time. There are a number of dome and volcanic cones made-up of both

basic and felsic volcanic rocks of Plio-Quaternary age. The subsurface equivalents of the felsic domes and volcanic rocks may be the hypabissal intrusions, and they have not been unroofed yet. From this point of view, it is sugested that the heat source of the DGF, which is located at foot of the Tendürek polygenetic volcano and near by the Taşlıçay granitoid, may be such kinds of felsic hypabyssal intrusions.

3.1.5. Dalören Volcanic Rocks

These volcanic rocks are exposed widely to the southern margin of the DGF (Figure 3). The full volcanic succession, its synsedimentary (e.g., growth faults) and deformational structures (e.g., conjugate fractures and folds) are observed well around Aşağı and Yukarı Dalören villages (Figure 7). These settlements are outside of the study area but very close (at 1 km away) to the southern margin of the DGF. For this reason, this folded volcanic sequence was termed as the Dalören volcanic rocks in the present study. The Dalören volcanic rocks are composed mainly of rhyolite, andesite, trachyandesite, basaltic andesite, basalt and related pyroclastites (e.g., mostly ignimbrite, tuff and tuffite). The bottom of the Dalören volcanic rocks are not seen in the study area. However, it is observed well around Apro settlement to the southwest but outside the study area. At this locality, both the Kendel metamorphic rocks and the Taşlıçay granitoid are overlain with an angular unconformity by the Dalören volcanic rocks. The volcanic sequnce begins with the volcanic breccia and tufss onto the erosional surface of the older rocks, and then continues upwards with the alternation of ignimbrite, andesite, tuff, rhyolite, trachyte and volcanic breccia. At the topmost, the sequence is covered by a thick-bedded to massif ignimbrite horizon. In addition, the Dalören volcanic rocks display both erosional stratigraphical and also thrust-faulted contact relationships with the Pliocene Mutlu faormation. Tuff and tuffites are white, yellow, and green in color, thin bedded to laminated and not resistent to the weathering processes.

Therefore they display gentle topographic slope and can be easily recognized away from outcrop. In contrast to them, the ignimbrites are thick-bedded (up to 2m) to massif, dark browen to red in color and very resistent to the weathering. They are cut across frequently by vertical cracks, thus they display vertical to sub-vertical columnar structure and very steep scarps (up to 15 m high). The Dalören volcanic rocks are folded and cut across by the neotectonic structures (e.g., oblique-slip normal faults and strike-slip faults), In addition, they are overthrusted from north to south on the Pliocene Mutlu formation in places (Figure 8). The total thickness of the Dalören volcanic rocks is 700 m. Based on both the isotope and geochemical data, the origin of the Dalören volcanic rocks is a partly contaminated hybrid magma formed by the partial melting of lithospheric mantle (Keskin, 2003; Açlan and Turgut, 2017; Açlan and Duruk, 2018; Kansun et al., 2020). Consequently, the Dalören volcanic rocks have an impermeable texture due to the weathering. For this reason, they are one of the significant cover rocks of the DGF.

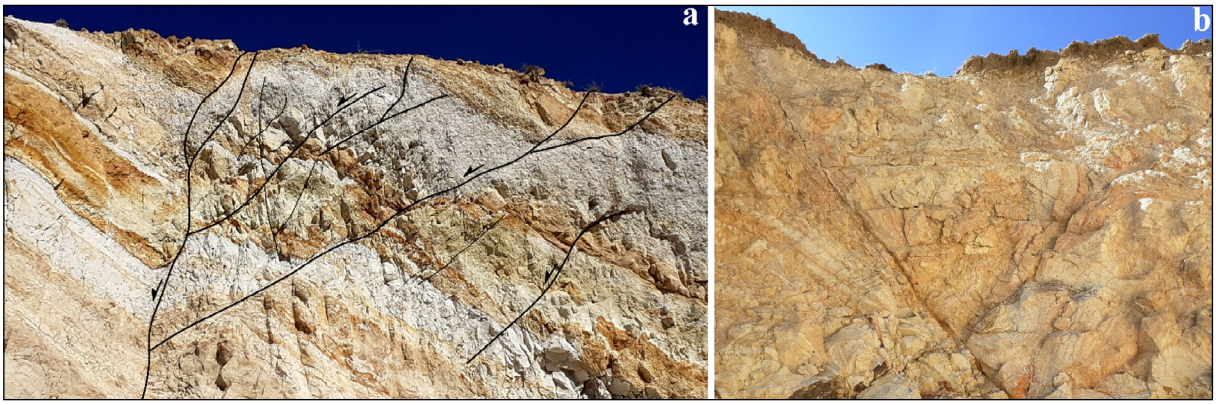

Figure 7- a) Close-up view of the normal growth-faulted tiffite of the Upper Miocene Dalören volcnic rocks (eastern limb of the Burgulu anticline), b) close-up view of intensely fractured (single shear planes and conjugate fractures) tuff-tuffite of the Dalören volcanic rocks.

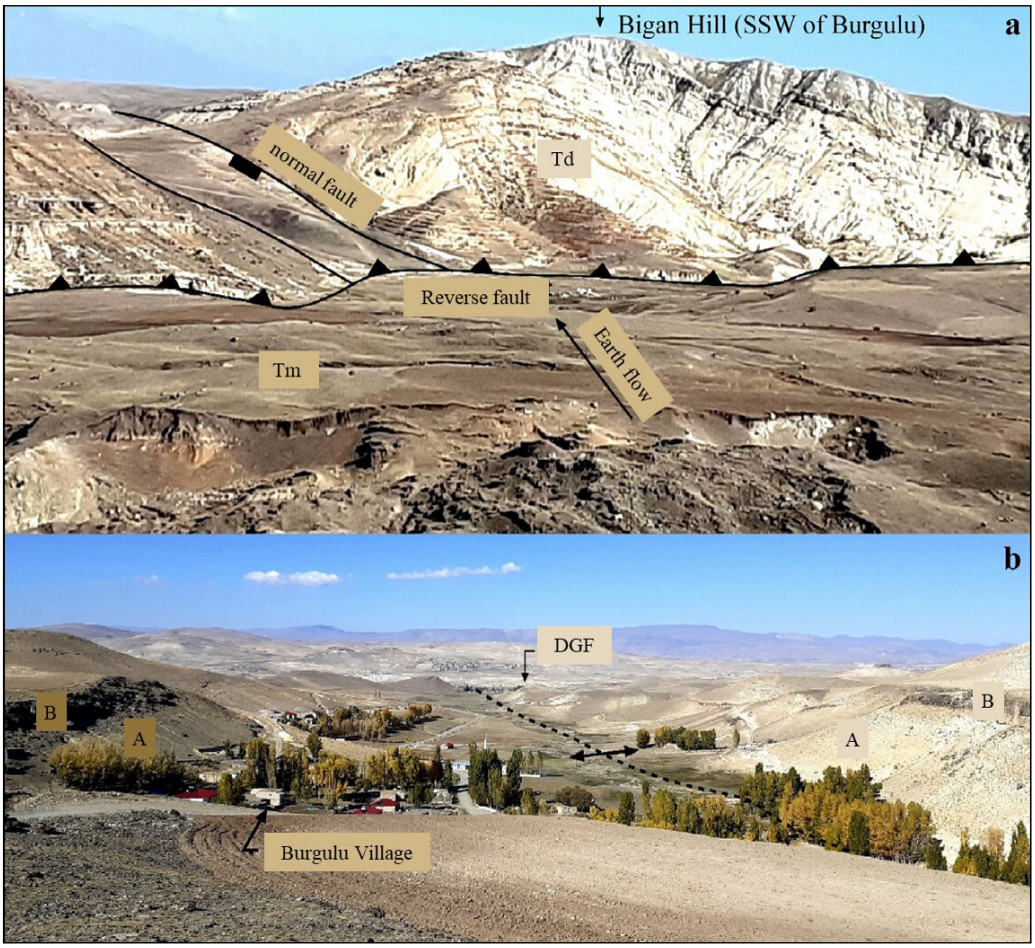

Figure 8- a) General view of the tectonic contact (reverse fault) between the deformed (folded and oblique-slip normal-faulted) Dalören volcanic rocks (Td) and the Pliocene Mutlu formation (Tm) under the threatening of earth flow, SSW of the Burgulu Village (view to N), b) General view of the burgulu anticline with an approximately N-S trending axis. A. tuff-tuffite, B. ignimbrite, DGF. Diyadin geothermal field (view to N).

3.1.6. Mutlu Formation

In general, the Mutlu formation is represented by a loose and 400 m thick volcanosedimentary sequence of Pliocene age. It is exposed in a relatively small area to the near east-northeast of the Diyadin County in the study area. In contrast, it is the most widespread unit in the area, approximately 2-3 km away from the southern margin of the DGF, i.e., its major outcrops are observed around Mollakara, Aşağı-Yukarı Dalören, Mutlu, Gedik, Saitbeyli, Yolcupınarı, Gözüpek and Oğuloba villages to the south and outside the DGF (Koçyiğit, 2022). At the bottom, the Mutlu formation overlies with an angular unconformity the erosional surface of the Kendel metamorphic rocks. The top of the Mutlu formation is mostly free erosional surface, but some times it is a faulted contact with both the older and younger rocks units owing to the multiple deformation it experienced. Particularly, the top contact of the Mutlu formation is in the nature of thrust to reverse fault with the folded Dalören volcanic rocks of Miocene age (Figure 8). The Mutlu formation begins with a ten meters thick polygenetic to unsorted basal conglomerate on the erosional surface of the Kendel metamorphic rocks at the bottom, and then continues with the alternation of pebble-supported coarse-grained sandstone, siltstone, mudstone, tuff, tuffite, basaltic scoria, obsidian and claystone. The topmost of the sequence is covered by a loose conglomerate-sandstone alternation. Major clasts of basal conglomerate are marble, dolomite, quartzite, calcschist, granite, andesite, rhyolite, basalt and ignimbrite. They are sub- to well-rounded and range from 2 cm to 1.5 m in diameter. They also display

pebble imbrication. One of the major characteristics, which makes the recognition of the Mutlu formation easy, is the widespread earth flows took place within the formation owing to the secondary clay mineralization of claystones included in, and the oversaturation of the loose structure of the Mutlu formation. The second major characteristics of the Mutlu formation is the 3 m-150 m wide and iron-rich alteration zone (Figure 9). It occurs along and nearby the erosional contact separating the overlying Mutlu formation from the underlying marbles of the Kendel metamorphic rocks. From this point of view, this alteration zone reveals, from one hand, the existence of the subsurface geothermal fluid, from other hand, the key role of the Mutlu formation in the development of the DGF, because it is another cover rock of the DGF.

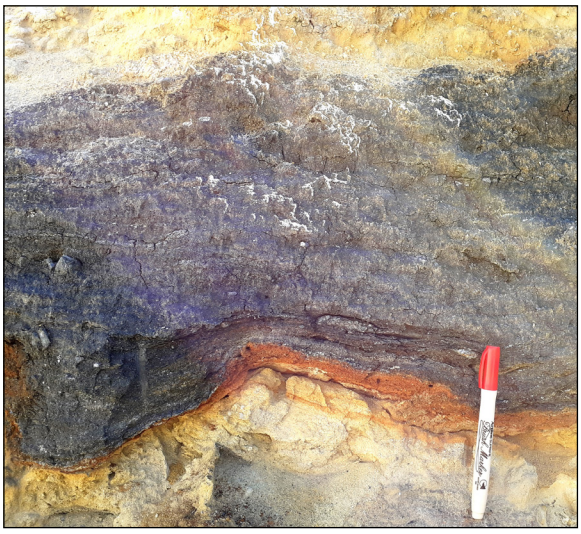

Figure 9- Close-up view of the irone-rich geothermal alteration zone formed in the marble of the Kendel metamorphic rocks close to the erosional bottom contact of the overlying Mutlu formation (SW of Ulukent Town).

3.2. Neotectonic Units: Major Manifestations of DGF

3.2.1. Diyadin Volcanic Rocks

They are exposed in a 0.2-1 km wide, 18 km long and NNW trending belt located between the Kale Hill in the south-southeast and the Omuzbaşı village in the north-northwest (Figures 3 and 4). The Diyadin volcanic rocks are composed of two sections. The lower section consists of basaltic breccia, lapilli, scoria, volcanic glass (obsidian) and tuff in a total thickness of 30-100 m. It is overlain with a sharp contact by the basaltic lava flow, i.e., the upper section of the Diyadin volcanic rocks (Figure 10a). It is dark black in color

Figure 10- a) Close-up view of the Diyadin volcanic rocks of Plio-Quaternary age. A. tuff-tuffite, B. volcanic breccia, and C. Columnar basalt, b) general view of the densely fractured basaltic columnar structure comprising the eastern wall of the Murat canyon (view to E).

and has a total thickness of 40 m. The basaltic lavas are densely fractured and display columnar to flow structures (Figure 10b). They are composed of several phenocrysts such as olivine, pyroxene (augite), apatite and some opaque minerals set in a finer-grained matrix made-up mostly of pyroxene microliths.

In general, the Diyadin volcanic rocks are underlain by the NNW trending open fracture termed here as the Kaletepe open fracture (KOF in Figure 1b). The first volcanic activity in and adjacent to the DGF initiated across two eruption centers, namely the Kaletepe eruption centers, situated at the SSE tip of the KOF around the Davutlar village at the southeast corner of the DGF (Figure 3). The olivine basaltic lavas were poured out of these two eruption centers and then started to flow in down-slope direction up to the Omuzbaşı village by using the KOF, thus the columnar olivine basalts formed by the cooling and solidification of this basaltic lava. The Diyadin volcanic rocks display thermal contact relationships with both the Upper Miocene Dalören volcanic rocks and the Pliocene Mutlu formation, i.e., Diyadin volcanic rocks are relatively younger than them. However, they show gradual top contact relationship with the Plio-Quaternary Göğebakan travertines (Figure 2). For this reason, the relative age of the Diyadin volcanic rocks is Plio-Quaternary. The alkali olivine columnar basalts are also very widespread rocks exposed in Malazgirt (Muş), Tutak (Van), Patnos and Hamur (Ağrı) regions within the east Anatolian tectonic block (EATB) (Türkecan et al., 1992; Esirtgen and Hepşen, 2018; Sümengen, 2009). The radiometric ages of the columnar basalts in these regions are 1.07 ± 0.12 my (Sanver, 1968), 2.0 ± 0.1 my and 3.9 ± 0.4 my (Innocenti et al., 1980), respectively. Consequently, the relative age of the Diyadin volcanic rocks is more or less same as the radiometrik age of these columnar basalts.

The Diyadin columnar basalt is one of the major manifestations of the DGF. Because, it is the production of first fissure eruption in the Diyadin region which triggered the onset of other eruptions and let to the development of nearby Tendürek polygenetic volcano (Figure 1b). In the same way, this event is also the initial key for the development of the strike-slip neotectonic regime and the Diyadin geothermal field. In addition, after this first fissure eruption and formation of the Diyadin columnar basalts, the upstream section of the 722 km long Murat River, which is one of the major branch of the Fırat drainage systemin in the east Anatolia, was settled down along the KOF and carved its bed deeply into the basalts and resulted in a 40 m deep and very narrow canyon, namely the Murat Canyon, during the development of the DGF under the control of strike-slip neotectonic regime. In the present, the Diyadin County is located on the eastern wall of this outstanding morphotectonic structure (Figure 11).

3.2.2. Göğebakan Travertines (Fossil travertines)

This unit was previously mapped and interpreted as a lacustrine limestone by Esirtgen and Hepşen (2018) and Kansun et al. (2020). In contrast to their interpretation, in the present study, it was identified that it is an older travertine deposited by the thermal fluids in the forms of plateau-, terrace-, mound- and

Figure 11- General view of the Murat canyon and the Diyadin County situated on its eastern wall (view to E).

fissure-ridge travertines within the DGF. Even though these travertines have lost the most of their original physical features due to the erosional period they have experienced, their original internal structures can be still observed inside the mining quarries opened in older travertines (Figure 12). In the present study, these older travertines were renamed as the Göğebakan travertine by the name of their type locality (Göğebakan village).

The Göğebakan travertines are the most widespread unit in the DGF (Figures 3 and 4). They cover an area of several tens of km². They show faulted- to erosional contact relationships with the pre-late Pliocene rocks. In contrast, the contact relationship between the Diyadin volcanic rocks and the Göğebakan travertines is conformable. For this reason, the relative age of the Göğebakan travertines is at least Plio-Quaternary. In general, the Göğebakan travertines are composed mostly of medium- to thick-bedded, but rarely massive travertines crossed frequently by open fractures. Total thickness of the Göğebakan travertines is 200 m.

3.2.3. Yeşildurak Formation

This unit is exposed well around Kardeşli, Yeşildurak and Aşağısaatçılar villages along the east-northeastern margin of the Akpazar pull-apart basin (Figures 4a and 4b). It overlies with an angular unconformity the serpentinites of the Kardeşli ophiolitic mélange (Figure 6) and the Paleocene-Eocene Harapköy formation at the bottom (Figure 5). However, it displays an overturned contact relationship with the Paleocene-Eocene Harapköy formation in places (Figure 4b). In general, it shows both the gradual and faulted-contact relationships with the Quaternary basin fill. At the bottom, it begins with the unsorted to polygenetic conglomerates, and then continues with the alternation of sandstones, mudstone, marl and again conglomerates (Figure 13a). Conglomerates are weakly lithified to loose and consists of sub-rounded to rounded clasts of mostly marble, limestone, serpentinite, quartz, andesite, basalt, granite, ignimbrite, chert, radiolarite, diabase (Figures 13b). They range from 2 cm to 75 cm in diameter. They set in a sandy matrix bounded weakly by both calcite and silica cement. Total thicknes of the sequence is 60 m. The yeşildurak formation is nearly flat-lying except for the area adjacent to the active faults. For istance, they are tilted up to 20° and overturned along the northern margin-boundary fault, the Murat fault (Figures 4 and 13a).

Figure 12- Close up view of the internal structure of the Göğebakan travertins (near ENE of the Göğebakan Village).

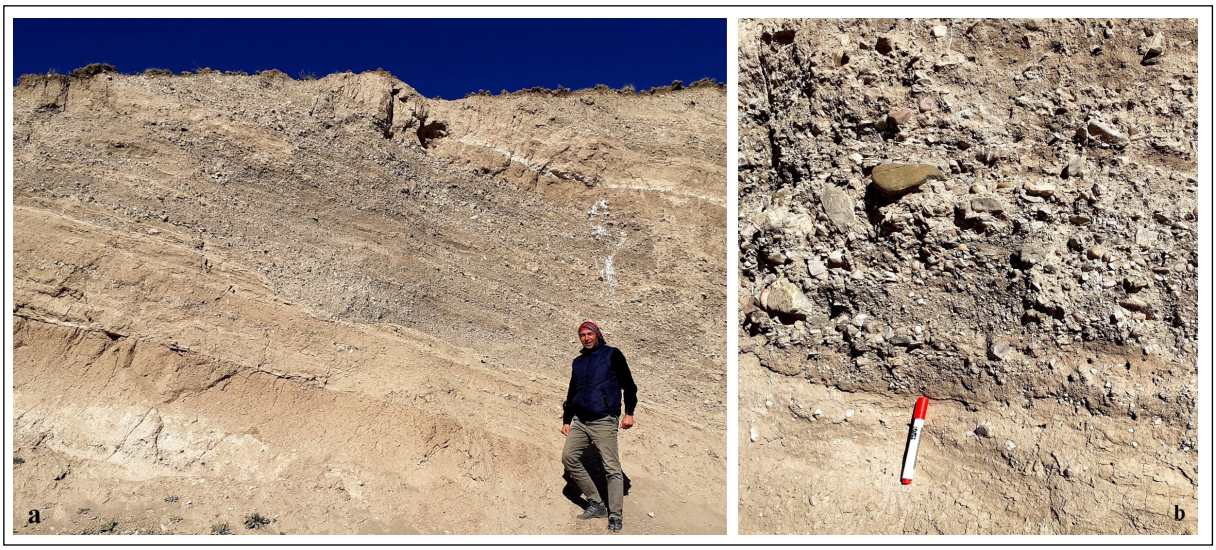

Figure 13- a) General view of the tilted Yeşildurak formation exposed against the active Murat fault, b) Close-up view of the sharp contact between the underlying mudstone and overlying polygenetic to unsorted conglomerate horizon.

3.2.4. Tendürek Volcanic rocks

The final continent-continent colision and formation of the Bitlis suture zone between the northerly located Eurasian and southerly-located Arabian plates were also accompanied by a post-colisonal volcanic activity of dissimilar chemical composition (Pearce et al., 1990; Ölmez et al., 1994; Yılmaz et al., 1998; Lebedev et al., 2016). This volcanic activity lasted untill the historical times with the occurrence of a series of isolated volconic cones such as Nemrut, Süphan, Tendürek and ağrı volcanoes situated in EATB. The Nemrut, Süphan and Ağrı are the stratovolcanoes formed by the alternation of both pyroclastites and lavas. In contrast to them, the Tendürek is a double-peaked strato-shield volcano covering an area of 650 km². The Tendürek volcano is located in an extensional area provided by the Ağrı, Balıkgölü and Çaldıran fault zones to the near east-southeast of the DGF (Figure 1b). The heights of greater and lesser Tendürek volcanoes are 3549 m and 3319 m respectively (Lebedev et al., 2016). The Tendürek volcano is composed mainly of trachytic lavas-pyroclastites (volcanic breccia, lapilli, tuff) and basaltic lavas to related pyroclastites (volcanic breccia, pumice and obsidian). The total thickness of volcanic sequence is about 1.7 km (Yılmaz et al., 1998). The volcanic sequence rests on both the Paleozoic Kendel metamorphic rocks and the Upper Cretaous east Anatolian accretionary prism (EAAP) at the bottom. The first volcanic activity started with the fissure eruption along the polygenetic Lesser Tendürek stratovolcano and then continued througout the Greater Tendürek shield volcano. The Lesser Tendürek volcano consists of both basic and felsic lavas, while the Greather Tendürek volcano is composed of intermediate to mildly felsic lavas. The present morphology of the Tendürek volcano has formed at five phases during the time slices of 250-200, 200-150, 150-100 and 50 thousand years before present (Lebedev et al., 2016). The Tendürek volcano is at the stage of caldera crossed and deformed by a seris of concentric to radial faults (open fractures). Widespread occurrence of gas and steam outputs (fumaroles) at the foot of the Tendürek volcano and the numerous hot water springs included in the nearby DGF reveal that it is still active in the present. In addition, based on the ratio of C- and He- istopes (C13/C12; He3/He 4), the origin of the gases coming out of the Tendürek volcano is mantle (Ölmez et al., 1994). Consequently, the active Tendürek volcano is another manifestation of the DGF (Figure 1b).

3.2.5. Diyadin Thermogene Fissure-Ridge Travertines

The most diagnostic manifestation of the DGF is the actively growing thermogene fissure-ridge travertines (Figure 3). Travertines are resulted from the deposition of the calcium- and bicarbonate-rich cold to hot waters coming out of the Earth by using the

open fractures, such as the normal faults, because they are the most suitable pathways for the circulation of ground waters. At depths, the CO_2 content of ground water is considerably high. For this reason, it makes the water oversaturated in CO_2, and thus inhibits both the precipitation of $CaCO_3$ and the formation of travertine. In contrast to the process at the depth, both the CO_2 and pressure suddenly release when ground water reaches to the ground surface. This makes the water unsaturated in CO_2, and thus the formation of travertine begins (Figure 14). In this frame, there is a close relationship between active faults and travertine occurrences. The fissure-ridge travertine is one of the most significant recorders of the neotectonic activity (Altunel and Hancock, 1993; Altunel, 1996; Hancock et al., 1999; Altunel and Karabacak, 2005; Koçyiğit, 2005; Brogi et al., 2005; Karabacak, 2007; Mesci et al., 2008; Temiz et al., 2009; Pasvanoğlu, 2013; Koçyiğit and Doğan, 2016; Brogi et al., 2021; Koçyiğit, 2022). For instance, Hancock et al. (1999) proposed the term "Travitonics" to emphasize the close relationship between the travertine formation and active tectonics. Indeed, there is a kinematic relationship between the general strike of the central fissure plane and the operation direction of the greatest principal stress axis (σ1) if the fissure-ridge travertine has developed under the control of σ1. In the case of strike-slip tectonic regime, the strike of the fissure plane is more or less parallel to the σ1 (Brogi and Capezzuoli, 2009; Koçyiğit and Doğan, 2016; Doğan et al., 2019; Brogi et al., 2021), but it is perpendicular to it in the case of tensional tectonic regime and related normal faulting

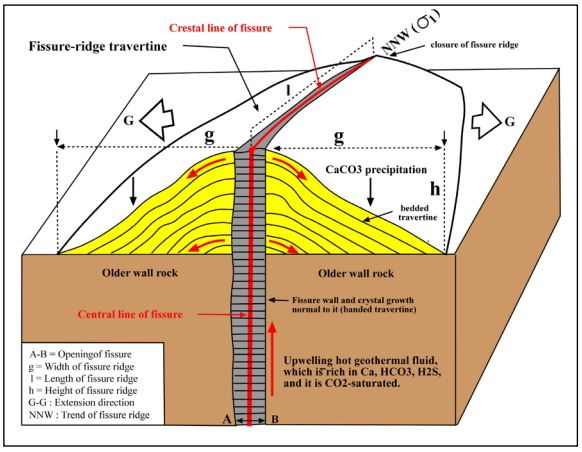

Figure 14-Sketched block diagram illustrating how the fissure ridge travertines are formed.

(Koçyiğit, 2005). The DGF is the type locality for the widespread fissure-ridge travertine occurrences. Therefore, fissure-ridge travertines in the study areas were first named as the Diyadin fissure ridge travertines (DFRT) and analyzed kinematically.

In general, except for several fissure-ridge travertines (Figure 4), most of them are situated in the area among Göğebakan, Taşbasamak, Günbuldu, Altınkilit, Dibekli, Tazekent and Davutköy villages and to the near south of the Diyadin County (Figure 3). For this region, this area was named as the Diyadin geothermal field (DGF). In the same way, the most of hot water springs and the shallow artesian wells are also located in the same area, i.e., the origin of the fissure-ridge travertines is hot water springs in the study area (Figures 3 and 14). Totally sixtyfive fissure-ridge travertines were mapped on 1/25.000 scaled map. They display a structural pattern like a doubly-plunging anticline (Figure 15a) with curvi-linear axis, which corresponds to the central fissure connecting a series of spring orifices (Figure 15b). Their sizes range from 160 m to 1200 m in length (maximum), from 6 m to 36 m in height, and from 66 m to 500 m in width, respectively.

In the same way, the openings of the central fissures range from 10 cm to maximum 13 m where the calcite crystals were grown in a direction normal to the walls of central fissures (Figures 14, 16a, 16b). They trend in N-S, NNE (up to 25°), NNW, NW (up to 65°), WNW and ENE directions. Some of the fissure-ridge travertines are conjugate in pattern where the vertical to sub-vertical open fractures of the fissure-ridge travertines intersect to each other under acute angles. The North East Anatolia (EATB) and the northwest Iran are seismically active regions deformed by both the strike-slip and thrust faulting sourced from the strike-slip neotectonic regime (Koçyiğit, 2013; Moghoori et al., 2021). These authors also determined that the stress field state in the same region is being dominated by N158° (N22°W) trending greatest horizontal compressive stress axis (σ1), sub-vertical intermediate stress axis (σ2) and the N068° (N68°E) trending least principal stress axis (σ3) by using the tensor solution diagrams of the 277 earthquakes took place in the same region. Based on this stress field state, the NNW, NW- NE- and ENE trending faults are the oblique-slip normal, dextral strike-slip, sinistral

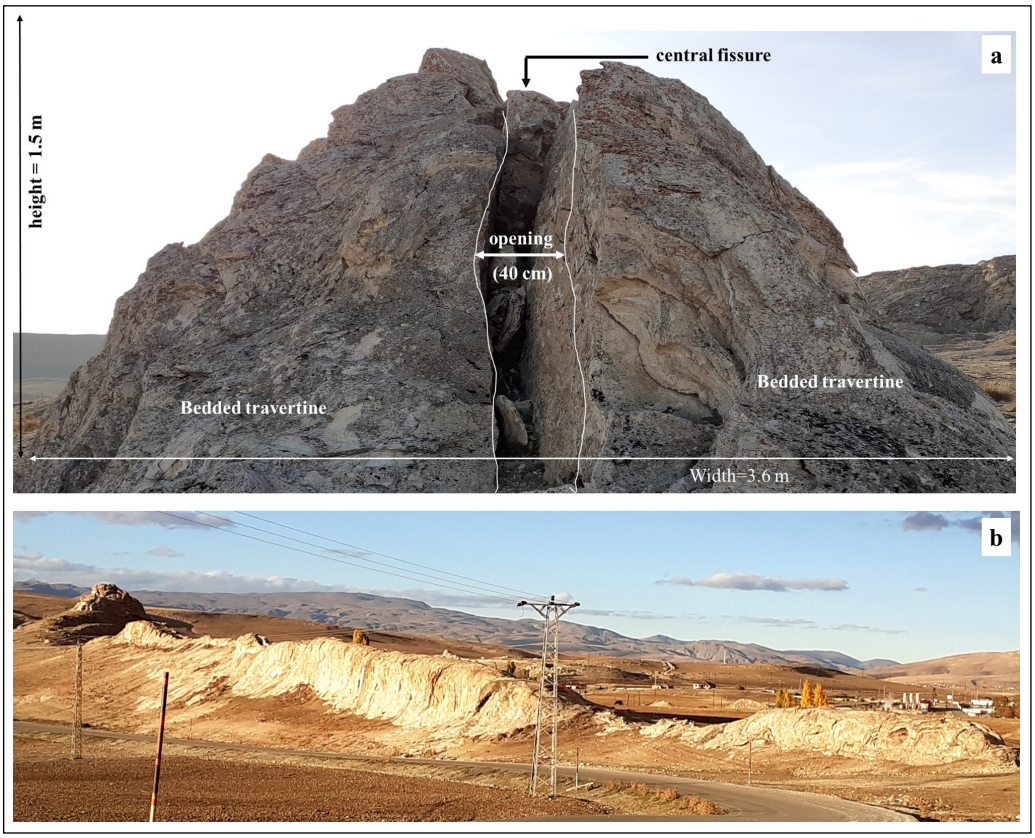

Figure 15-a) Cross-sectional view of the N50W trending fissure-ridge travertine (near north of Yılanlı thermal (YT in Figure 3), b) General view of the N50°W trending Yılanlı fissure-ridge travertine (view to NNE).

strike-slip and the thrust-to reverse faults, respectively. As is seen on geological maps (Figures 3 and 4), the fissure-ridge travertines formed not only along the NNW trending open fractures (normal faults), but also along the NW trending dextral to NE trending sinistral strike-slip faults and approximately ENE trending reverse faults, i.e., the DFRT are multi-directional based on the strikes of fissure-ridge axial planes. This occurrence pattern of the fissure-ridge travertines may imply to the abundance and high sub-surface pressure of the geothermal fluids in the DGF.

The fissure-ridge travertine deposits in the study area have not been dated radiometrically. However, they must be the late Pleistocene to Holocene in age based on the stratigraphical relationships among the travertine occurrences, the Plio-Quaternary columnar basalt and terrace deposits in the DGF (Figures 3 and 4). For instance, the fissure-ridge travertines show gradual contact relationships with the basin floor sediments of the late Quaternary age, while they cut across the Plio-Quaternary Diyadin columnar basalts (Figure 17), i.e., the relative age of the fissure-ridge travertines must be the late Quaternary-recent, because their formation is still lasting in the areas, where the level of regional water table is above ground surface.

In general, from the plate tectonic configuration point of view, fissure-ridge travertines are concentrated not only along the active plate boundaries, but also in both sides (out-and inside) the plate boundaries throughout the territory of Türkiye. The common and well-defined examples of them are as follows: (1) the Reşadiye fissure-ridge travertines (Mesci et al., 2020), (2) Akkaya (Eskipazar-Karabük) fissure-ridge travertines (Yıldırım, 2018), (3) Karakoyun-Yoğunağaç (Elazığ) fissure-ridge travertines (Kalender et al., 2015), (4) Sıcak Çermik (Sivas) fissure-ridge travertines (Mesci et al., 2008; 2018), (5) Kızıltepe (Avcıköy) and Sarıhıdır-Balkayası (Avanos) fissure-ridge travertines (Atabey, 2002; Koçyiğit and Doğan, 2016; Karabacak and Mutlu, 2019; Temiz et al., 2021), (6) Kırşehir fissure-ridge travertines (Atabey, 2002; Temiz et al., 2009), (7) Yaprakhisar-Ziga fissure-

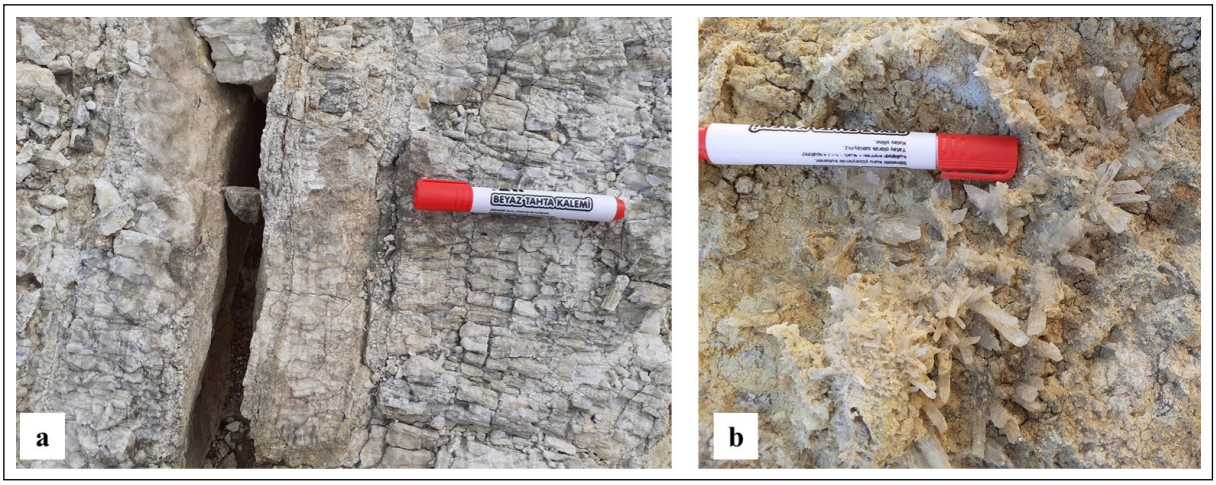

Figure 16- a) Close-up view of calcite minerals grown in a direction normal to the walls of the central fissure, b) Close-up view of calcite crystals.

ridge travertines (Doğan et al., 2019), (8) Urganlı (Manisa) fissure-ridge travertines (Demirkıran and Elçi, 2022), (9) Akhüyük (Ereğli-Konya) fissure-ridge travertines (Şener, 2018; Temiz and Savaş, 2018), (10) Hamamboğzı (Banaz) fissure-ridge (Koçyiğit, 2008), (11) Karahayıt-Pamukkale-Kaklık (Denizli) fissure-ridge travertines (Özkul et al., 2002; Koçyiğit, 2005; De Filippis et al., 2013; Özgür et al., 2017; Van Noten et al., 2018), and (12) Çamlık and Dereiçi (Başkale-Hakkari) fissure-ridge travertines (Sağlam-Selçuk et al., 2017; Yeşilova, 2021). The first two examples are located along the plate boundary, namely the NAFS, i.e. they are strike-slip faulting-induced fissure-ridge travertines. The examples 3 through 8 are intra-plate fissure-ridge travertines formed under the control of again active strike-slip faulting. The examples 9, 10 and 11 are also intra-plate fissure-ridge travertines, but they have developed under the control of tensional tectonic regime, in which the greatest principal stress axis (σ1) is sub-vertical in state. The last one, the example 12, is located in the EATB, and it's all characteristics are more or less same with those of the DFRT. The description of all these fissure-ridge travertines is outside of the paper. For this reason, readers, who are interested in fissure-ridge traverines, are kindly invited to see the above-mentioned papers and other literatures therein.

In general, one of the most diagnostic ground surface manifestations of geothermal fields is the thermogene fissure-ridge travertine. Recently, two well-defined fissure-ridge travertines were reported

Figure 17-General view of the N-S trending vertical fissure-ridge travertine (B) cutting across the Plio-Quaternary Diyadin columnar basalt (A) (eastern wall of the Murat Canyon).

from Italy, and introduced to the international literature. These are the Terme San Giovanni fissure-ridge travertine (Brogi and Capezzuli, 2009), and the Colle Fiorito fissure-ridge travertine (De Filippis et al., 2013). The first one is located in the Rapolano Terme area along the western margin of the Plio-Quaternary Siena basin shaping the interior side of the north-western Apennine chain. The second one is located at the southeastern tip of a NW-trending depression or paleograben (the Acque Albule Basin) drained by both the Tiber (Tevere) and Aniene Rivers cutting across the Roman magmatic system in the Tyrrhenian back-arc region or Tuscan geothermal field. Both of these fissure-ridge travertines have been formed along the normal faults under the control of a prominent

tensional tectonic regime accompanied secondly by the dextral strike-slip tectonic regime (Brogi and Capezzuli, 2009; De Filippis et al., 2013; Mancini et al., 2014; Porta et al., 2017; Vignaroli et al., 2020). The DFRT can be correlated with both of these two fissure-ridge travertines based on the age, hydro-chemical composition, morphology and the close-relationship with the active volcanoes. However, there are two basic contrasts among them: (1) The DFRT has developed in a pull-apart basin under the control of strike-slip neotectonic regime and related faults, (2) this fissure ridge travertine is multi-directional in the nature of it's strike of crestal fissure. In contrast to the DFRT, both the Terme San Giovanni fissure-ridge travertine and the Colle Fiorite fissure travertine are unidirectional and they have developed along the traces of active normal faults under the control of a tensional tectonic regime.

3.2.6. Thermal Springs and Artesian Wells

Recently a detailed geological to geochemical studies have been carried out on the natural mineral waters in both the central and periferal counties, such as Hamur, Patnos, Taşlıçay, Diyadin, Doğubayazıt, and Elekirt, of the city of Ağrı (Üçgün et al., 2014; Üçgün, 2019). They determined 37 thermal springs. 12 of them are in the nature of geothermal, the rest 25 are normal natural water springs. In addition, 15 of them are located in the Diyadin district. More or less, all of the hot water springs (Figure 18) and the artesian types of boreholes are concentrated in an approximately triangular area among Davutköy, Göğebakan and Tazekent villages (Figure 3) called so that "Diyadin Kaplıcaları" (Üçgün et al., 2014). Indeed, they are more widespread at four localities in this area. In terms of their names, these hot water springs were locally named as the Tazekent, Davutlar, Yılanlı and Bridge thermals respectively (TT, DT, YT and BT in Figure 3). The outlet temperatures of both hot water springs and wells range from 37°C to 78°C (Mutlu et al., 2013). Both the Yılanlı and Köprü thermals waters are also rich in sulfur. In a 35 m deep borehole drilled on the Mollakara-Gedik road (outside of the study area) passing along the western side of the Murat River flood plain, a hot water spring with the outlet temperature of 72°C erupted. In the present, hot waters of this artesian well are being used as an open air spa by the inhabitants of this region. In the same way, MTA drilled several boreholes with the depths ranging from 77 m to 215 m in the area between Yılanlı and Davutköy thermals (MTA in Figure 3). These wells also made artesian and hot waters with the outlet temperature of 62°C-78 °C poured out of the earth (Demirel and Özkan, 2000; Demir, 2006). Another borehole was drilled just on a NE trending fissure ridge travertine in the area very close to MTA wells (ABG in Figure 3), and a hot water with temperature of 65°C was obtained in the borehole at the depth

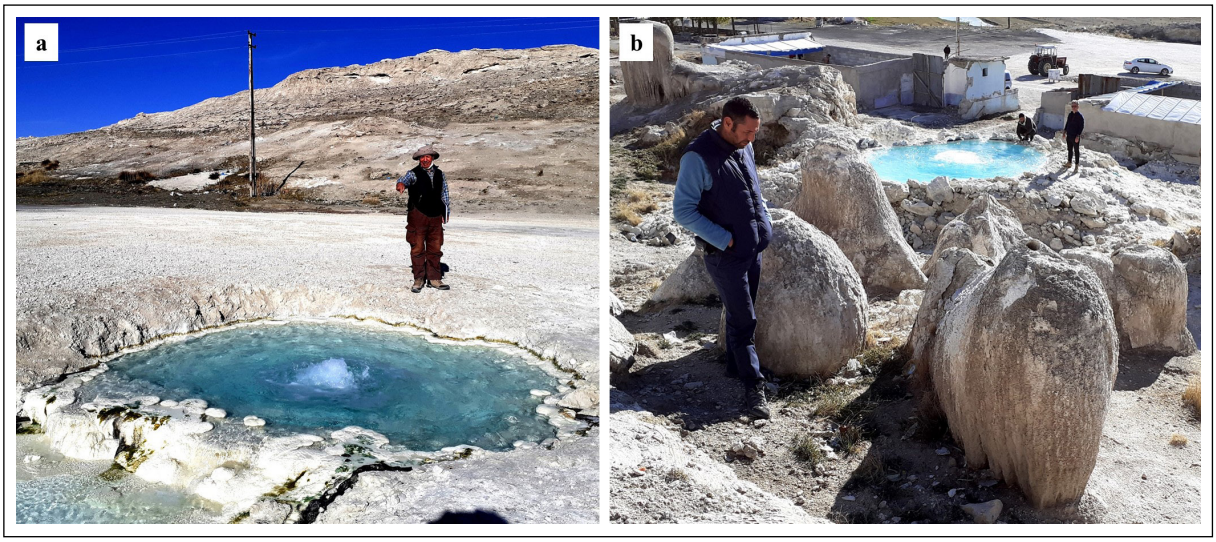

Figure 18- a) General view of a hot water spring with the outlet temperature of 50°C situated on the western side of the N50°W trending Bridge fissure ridge travertine in background (view to NE), b) close-up view of an again hot water spring among several mound-types of travertines up to 1.5 m high and 60 cm in diameter occurred at the same locality.

of 250 m. These waters are being used to heat the greenhouse (GH in Figure 3) constructed close to the well (Abdül Bahri Güzel, personal communication, 2021, Doğubayazıt). In general, hot and cold waters are in the composition of Na-HCO_3 and Ca-HCO_3 respectively. However, they also contain high amount of CO_2, H_2S and arsenic (As) in places. They are also meteoric in origin based on both oxygen- and hydrogen isotopes (Mutlu et al., 2013).

3.2.7. Quaternary Basin Fill

It consists of two major lithofacies based on their grain sizes and depositional settings. They are: (1) coarse-grained marginal facies, and (2) finer-grained basin floor facies. The marginal facies are represented by terrace deposits, older to recent superimposed alluvial fan deposits, and slope scree deposits. They are exposed widely along the fault-bounded margins of the Akpazar pull-apart basin (Figures 4a and 4b). Terrace deposits are observed well, in places, along the margins of the Murat River flood plain (Figure 3). The older flood plain deposits of the Murat River have been cut uplifted (up to 100 m) and then left as the fault terraces at different elevations (Figure 3). This observation reveals that both the flood plain of the Murat River drainage system and the margin-boundary faults of the Akpazar pull-apart basin are under the control of an active neotectonic regime. Alluvial fans show a fault-parallel aligned distribution pattern in different sizes ranging from several tens of m² to a few km². They consist of unsorted to polygenetic boulder blocks of mostly marble, schists, quartz, limestone, radiolarite, granite, diabase, spilite, ignimbrite, chert, and volcanic glass set in a sandy matrix at and nearby the apex of alluvial fans. Components of these loose conglomerate decrease in size and show a sorted texture towards the distal sections of alluvial fans. Some of the alluvial fans are in a superimposed pattern where older and larger fans are overlain by a number of smaller and younger alluvial fans. This pattern indicates that they have experienced a short term of non-depositional period followed by a sudden and high tectonic activity during their evolutionary history. One diagnostic example of these patterns is exposed well at the eastern tip of the Akpazar pull-apart basin (Figure 4b).

The second major lithofacies of the basin fill are composed of sandstone, siltstone, mudstone alternation with the intercalation of both the point- to mid-channel bar deposits, They show lateral and vertical gradational contact relationships with the organic material-rich claystone deposited in marsh and ponds. In addition, one of the largest fissure-ridge travertines (Akpazar fissure-ridge travertine) is included in the basin fill of the Akpazar pull-apart basin (Figure 4a). It is an about 1 km long, 200 m wide, 36 m high and trends N70°W direction. It cuts across the basin fill and still lasts to develop (Figure 19). Total thickness of the Quaternary basin fill ranges from 10 m to 100 m (maximum).

4. Akpazar pull-Apart Basin and Its Margin-Boundary Faults

In this region, the Akpazar pull-apart basin and its margin-boundary faults are other diagnostic manifestations of the DGF. It is drained by the Murat

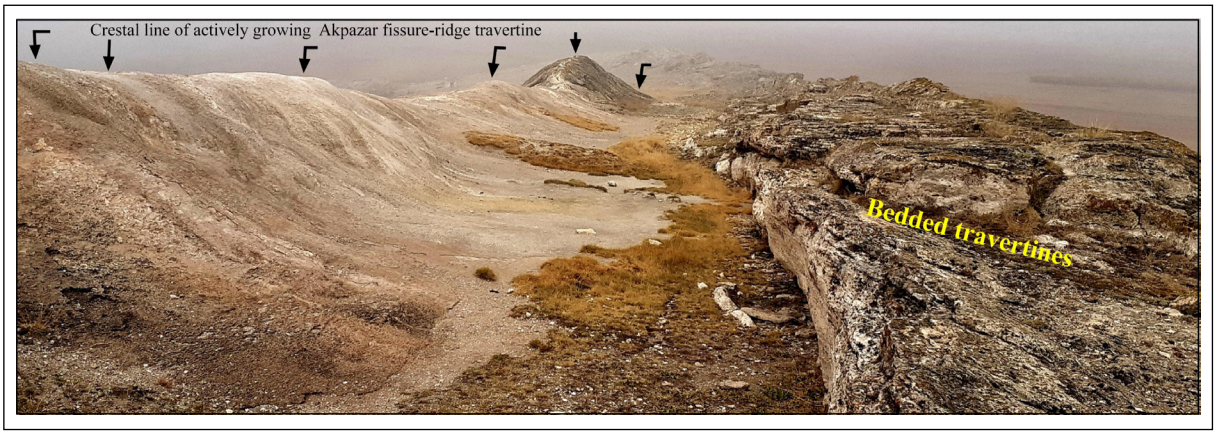

Figure 19- General view of the N70°W trending Akpazar fissure-ridge travertine (View to WNW).

River drainage system (Figure 4a). The Akpazar pull-apart basin is an approximately 17.2 km long, 0.5 -5.5 km wide and WNW trending depression of Quaternary age. It is situated between the Esen settlement to the west-northwest (Figure 4a) and the near east of Aşağısaatçılar village to the east-southeast (Figure 4b). The northern margin of the basin is more or less linear, while its southern margin is uneven in shape. For this reason the northern margin is determined and controlled by only one and linear structure, namely the Murat master fault (Figures 4a and b). In contrast to the northern margin, the southern margin of the Akpazar pull-apart basin is determined and controlled by a number of fault segments of dissimilar length, type and trend (Figure 4a). They trend in N-S, E-W, NNE, NW, NE and WNW directions, while their lengths range from 0.5 km to 9 km (maximum). Based on the stress field state in this region (Mokhoori et al., 2021), these fault segments are in different character such as normal, dextral to sinistral strike-slip, and reverse faults. The Quaternary basin fill of the Akpazar pull-apart basin is tectonically juxtaposed with various basement rocks of dissimilar age, lithology and deformation pattern by these fault segments along the southern margin of the basin. The longest fault segment bounding the southeastern margin of the Akpazar pull-apart basin is the Seyit fault. It consists of two segments cut and offset by another short and N-S trending fault segment (Figure 4a). These two segments are totally 9 km in length, and located in the area between Seyit village to the WNW (Figure 4a) and Çalışkan Village to the ESE (Figure 3). The southeastern segment of the Seyit fault displays northerly facing stepped land shape and juxtaposes tectonically Quaternary alluvial sediments with the Plio-Quaternary Göğebakan travertines. The linear fault trace, steep fault scarp and fault-parallel aligned earthflows (Figure 20) imply to the existence and activeness of the Seyit fault segments.

The eastern margins of both the Akpazar pull-apart basin and the DGF are determined and controlled by the Adakent fault zone (AFZ). It is totally 20 km long, 2-4 km wide and N-S trending active fault zone situated between the Taşkesen village to the south and near east of the Aşağısaatçılar settlement to the north (Figures 3 and 4b). The AFZ consists of numerous fault segments of dissimilar lengths, trends and character. These are the N-S trending normal, NW to WNW trending dextral strike-slip and NE trending sinistral strike-slip fault segments. The N-S trending fault segments are prominent structures. Lengths of the fault segments range from 0.2 km to 11 km (maximum). They cut across both the paleotectonic units and the Plio-Quaternary basin fill, and tectonically juxtapose them with to each other. In general, western blocks of fault segments comprising the Adakent fault zone were thrown downward up to 400 m.

The northern margin of the Akpazar pull-apart basin is bounded and controlled by the master fault (Murat fault) of the Ağrı fault zone, which was first identified and reported in this study. The Ağrı fault zone is an about 5-22 km wide, 120 km long and

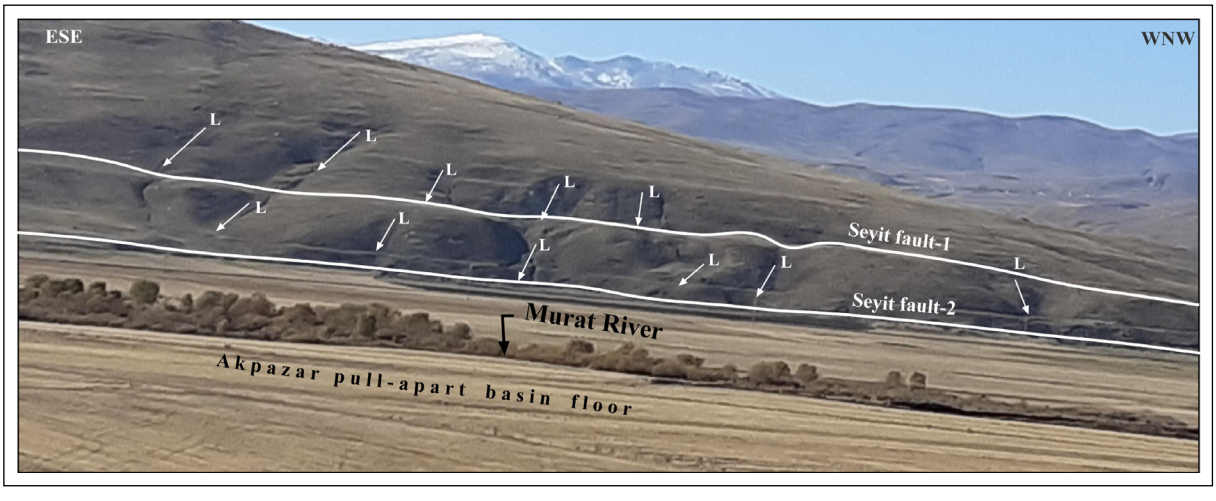

Figure 20- General view of the stepped Seyit faults, which bound and control southeastern margin of the Akpazar pull-apart basin (view to SSW). L. Earth flow.

WNW trending dextral strike-slip fault zone. It begins from the near north-east of the Eleşkirt County (Ağrı) to the west and outside of the study area, and then continues in ESE direction along the Ağrı pull-apart basin up to the Kumlubucak-Esen settlements, where it enters into the Akpazar pull-apart basin (Figures 4a and 4b). The Ağrı fault zone determines and controls northern margins of both the Ağrı and Akpazar pull-apart basins along its entire length. It consists of numerous, parallel to sub-parallel fault segments of different length, type and trend. The WNW trending dextral strike-slip fault segments are prominent. They cut across the Quaternary alluvial deposits, alluvial fans, stream beds and deflect to offset them in dextral directions. These relationships are observed well in the eastern section of the Ağrı pull-apart basin (Figure 21). In this area, the Murat River flows in WNW direction up to the city center of Ağrı, where it bends to SSE direction and exits the Ağrı pull-apart basin (Figure 21). In the eastern section of the Ağrı pull-apart basin, some sub-branches and their tributaries of the Murat River such as the Korşu stream and its tributaries, which flow in south direction along the northern margin of the basin, are cut, deflected and offset up to 21 km in dextral direction by the Ağrı fault zone and its master fault, the Murat fault, (A-A'= 21 km in Figure 21). This value indicates that the uniform slip rate along the Ağrı fault zone is 8.1 mm/yr (21 km/ 2.59 Ma = 8.1 mm/yr.) during the Quaternary neotectonic period. It also reveals that the magnitude of the peak earthquake to be sourced from the Ağrı fault zone is Mw = 6 or greater. To the near east of the Kumlubucak settlement, a N-S trending sill (highland) occurs and separates the easterly located Akpazar and westerly located Ağrı pull-apart basins from each other. However, the Murat fault cuts this high land and then continues up to 1 km northeast of the Omuzbaşı village where it jumps towards north and results in a left-stepping (restraining stepover) for 2 km distance around the Yeşildurak Village along the northern margin of the Akpazar pull-apart basin (Figures 4a and 4b). Here after, it runs in the same direction up to the near east of Aşağısaatçılar village, intersects with the N-S trending Adakent fault zone and then terminates at the easternmost tip of the Akpazar pull-apart basin (Figure 4b). The total length of the Murat fault in the study area is 17 km, and it consists of two segments. They determine and control the northern margin of the basin. As in the case of the Ağrı pull-apart basin, a number of alluvial fans of dissimilar size occur along the northern margin of the Akpazar pull-apart basin. They are also cut and deformed by the Murat fault (Figures 4a, 4b and 5).

5. Regional Fault Systems and Zones

These are the Tebriz (Tabriz), Erciş-Dorutay, Çaldıran, Ağrı, Balıkgölü (Gailatu), Siah Cheshmeh-Khoy, Iğdır, Aras and the Nakhichevan (Nahçivan) fault zones. Except for the Ağrı fault zone, remaining fault zones are situated outside of the study area. They have a key role in the development of the geothermal system in both the northwest Iran and northeastern Anatolia or EATB. For this reaon, their significant characteristics are described briefly below.

5.1. Tebriz Fault System

In general, the Tebriz fault system is an about 25 km wide, 210 km long, NW trending and seismologically very acctive dextral strike-slip fault structure. It is situated between the Bozkuş Mt. to the southeast and the near north-northwest of the Lake Urumiye to the norhwest (Figure 22). It consists of two major strands separated from one another by the intervening extensional right stepping (a pull-apart basin), where the City of Tebriz is situated (Figure 23) (Hessami et al., 2003; Aghajany et al., 2017). The western strand is known as the North Tebriz fault system, while the eastern one is termed as the South Tebriz fault system (Figure 22). Both the northwestern and southeastern sections of the North Tebriz fault system were moved by both the M 7.1 1721 and M 7.3 1780 historical earthquakes respectively; accordingly 35-50 km and 42-45 km long surface ruptures also occurred during these destructive earthquakes (Karakhanian et al., 2004). In addition, the slip rate on the North Tebriz fault system is 7 ± 1 mm/yr., and this value reveals that the return period of Mw 7.0 or greater earthquakes to be sorced from the North Tebriz fault system is between 250-300 yr. (Djamour et al., 2011). To the north-northwest of the Lake Urumiye, the North Tebriz fault system bifurcates into several fault zones, such as the Salmas, Erciş-Dorutay, Çaldıran, Balıkgölü-Siah Cheshmeh-Khoy, Iğdır, Aras and Nakhichevan fault zones, in the directions of E-W, WSW, NW and NNW, and then results in an extensional horse tail structures

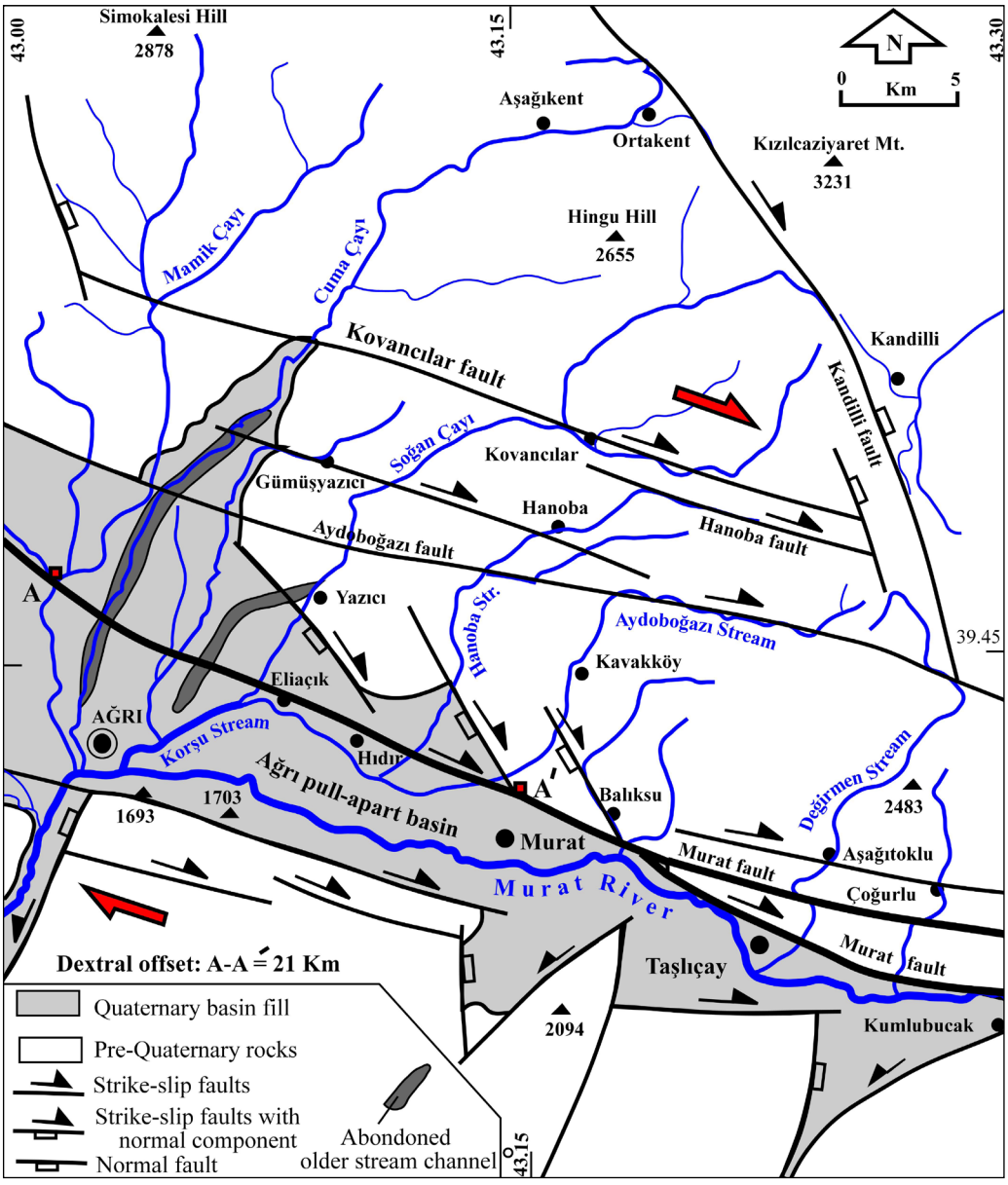

Figure 21-Neotectonic map of the eastern section of the Ağrı pull-apart basin and the offset drainage system (A- A'= 21 km) along the northern margin-boundary faults.

(Figure 22) (Copley and Jackson, 2006; Reilinger et al., 2006; Djamour et al., 2011). The most diagnostic menifestations of this extensional structueres are the DGF and the Tendürek to Ağrı volcanoes of Quaternary age. The most seismologically active one of these fault zones is the Çaldıran dextral fault zone, along which the motion on the North Tebriz fault system are being transferred towards northest Türkiye, i.e., into the EATB (Djamour et al., 2011).

5.2. Erciş-Dorutay Fault Zone

The Erciş fault zone is a 2-10 km wide, 90 km long and N40°-60°W trending active dextral strike-slip fault zone. It is located to the south and 45 km away from the study area It begins from the Patnos County to the northwest and outside the study area and then runs across the Erciş County, the Girekol, Etrüsk and Pirreşit volcanoes and Dorutay Town,

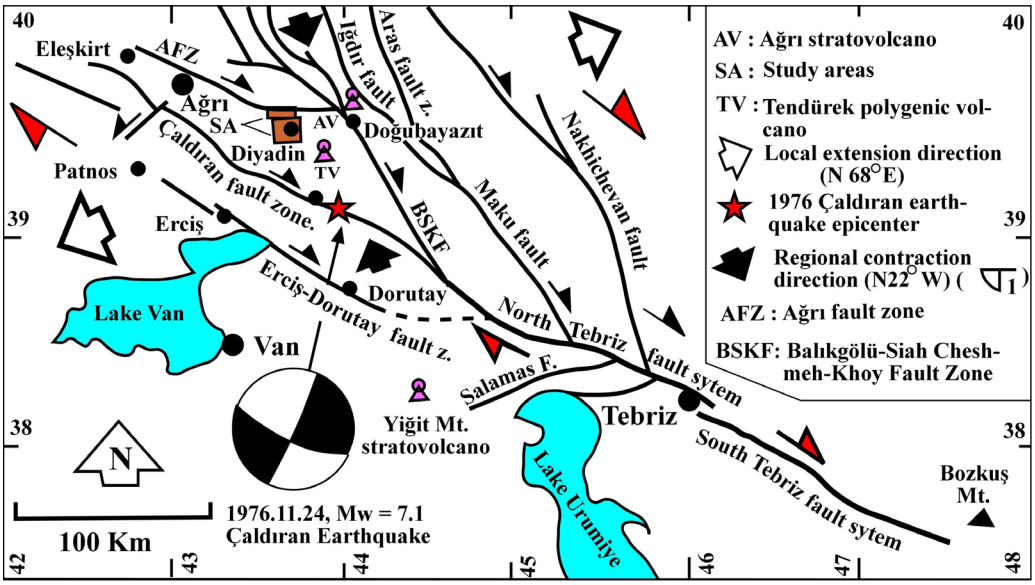

Figure 22-Simplified map illustrating the extensional horse tail structure (releasing type of horse-tail splay faults) in northeast Türkiye, Armania, Nakhichevan and northwest Iran.

Figure 23-General view of the Tebriz fault trace (F), its steep scarp and the city of Tebriz situated on the releasing stepover (view to N).

lastly. terminates near by the Turkish-Iranian State border to the southeast (Figures 22 and 24). The Erciş-Dorutay fault zone, which determines and controls the northeastern margin of the Van basin, consists of numerous, relatively short, parallel to sub-paralel and discontinuous fault segments of dissimilar length and trend. Among them the NW trending fault segments are prominent. The Erciş section was moved during the 23 October 2011 Tabanlı (Van) earthquake of Mw 7.2, and caused heavy damage and loss of life in these settlements (Koçyiğit, 2013). The small to intermediate seismic activity in and around this area are still lasting (Figure 24). Several stream beds (e.g., the Deliçay River) and alluvial fans are being cut, deformed and offset up to 850 m in dextral direction. Based on the offst morphotectonic features, the slip rate on the Erciş fault zone is 2.02 ± 0.12 mm/yr. (Sağlam-Selçuk and Kul, 2021).

5.3. Çaldıran Fault Zone

The Çaldıran fault zone was first determined and reported by Arpat et al. (1977). It is 2-8 km wide, 55 km long, N50°-80°W trending and northerly steeply dipping to convex dextral strike-slip fault zone. It begins from the Sarıkök settlement at the eastern foot of the Azizan volcano and then continues in southeast direction. Along its whole length it cuts across, in turn, the Kösedağ Volcano, the Hıdırmenteş sag pond, and the Çaldıran pull-apart basin, and offsets them in

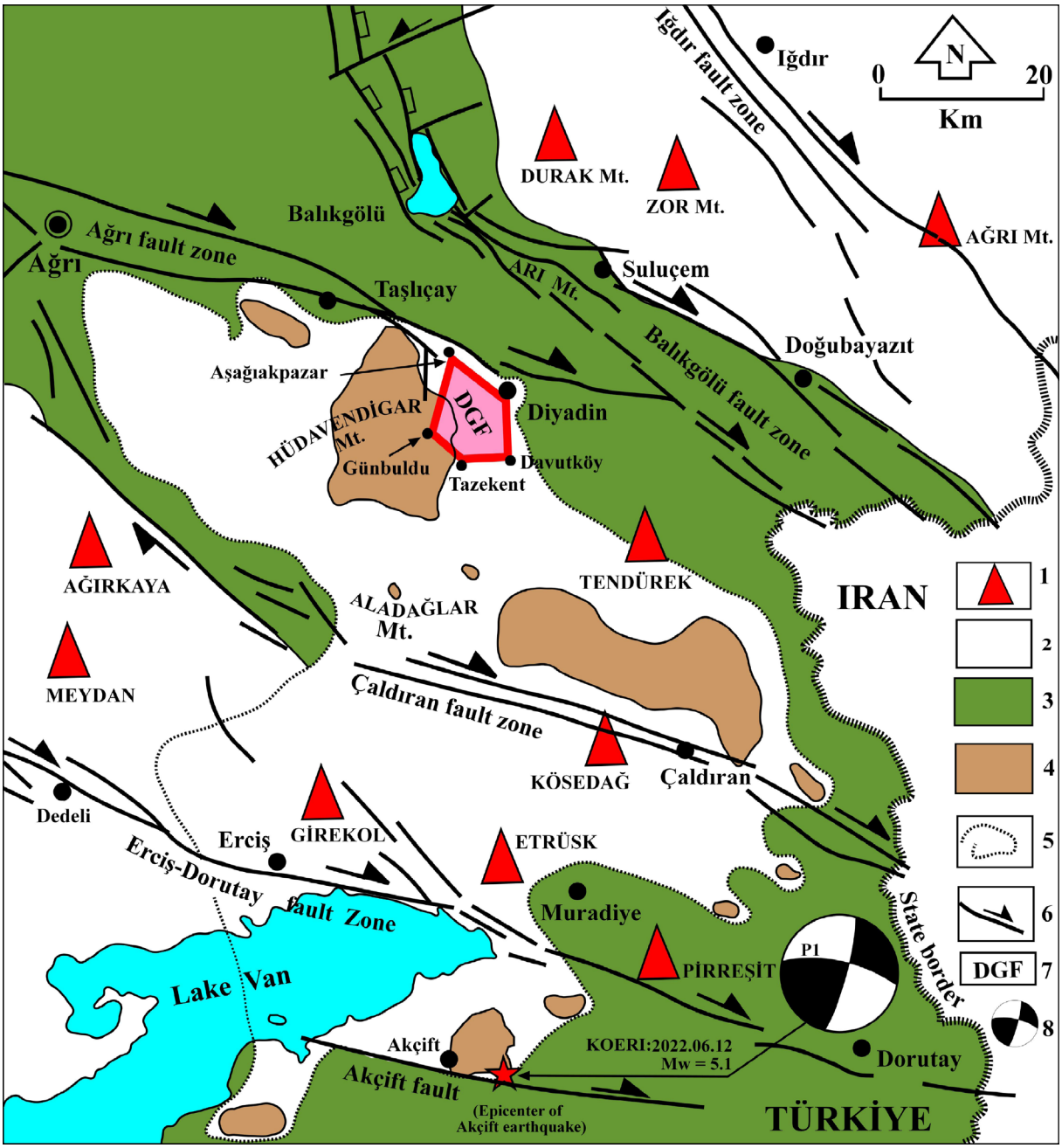

Figure 24-Simplified map illustrating distribution of both the reservoir and cover rocks of the geothermal system in eastern Anatolia. 1- isolated volcanic cones of Quaternary age, 2- post-collisional volcanic rocks sequence of late Miocene-Quaternary age, and the Neogene sedimentary sequence, 3- East Anatolian accretionary prism of Cretaceous-Paleocene age (EAAP), 4- Metamorphic rocks (Kendel metamorphic rocks) of Paleozoic age, 5-Approximate boundary of metamorphic rocks, 6- Active strike-slip fault zones, 7-Diyadin geothermal field and 8- Tensor solution diagram of Akçift earthquake (P1: source of earthquake-KOERI, 2022) (modified from Lebedev et al., 2016).

dextral direction. Lastly it joins with the North Tebriz fault system and terminates nearby the Gülderen to Baydoğan settlements at the Turkish-Iranian State border (Figures 1b and 22). The Çaldıran fault zone consists of numerous, parallel to sub-parallel, discontinuous fault segments of dissimilar length and trend. Along its whole length, the Çaldıran fault zone bifurcates and jumps to right and results in extensional steppings (releasing stepovers) such as the Dedebulak, Çaldıran and Siyahçeşme pull-apart basins (Figure 1b) (Şaroğlu et al., 1987; King and Nabelek, 1985; Sağlam-Selçuk et al., 2016). The Çaldıran fault zone was moved by the 24 December 1976 Çaldıran earthquake of Mw = 7.3 and led to the occurrence of an approximately 50 km long surface rupture with the coseismic dextral offset of 3.5 km (maximum) (Arpat et al, 1977; Toksöz et al., 1977; Ambraseys and Jackson, 1998; Tan et al., 2008). During the 1976 Çaldıran earthquake, whose epicenter is 25 km away from our study area, some settlements in the study area were heavily damaged. In addition, based on the GPS and morphotectonic data, both the Erciş-Dorutay and Çaldıran fault zones together were interpreted as the northwestern continuation of the North Tebriz fault system and reported that they are comprising the southwestern boundary of the Lesser caucasus-Talesh tectonic block moving in northeast direction (Copley and Jackson, 2006; Reilinger et al., 2006, Djamour et al., 2011). Same authors have also reported that the slip rate along this boundary, i.e., along the Erciş-Dorutay and Çaldıran fault zones, ranges from 7.2 mm/yr to 11mm/yr. In contrast to this values, it was determined and reported as the 3.27 ± 0.17 mm/yr based on the field geological data such as the offset formation boundaries (Sağlam-Selçuk et al., 2016). Based on a trench studies (paleoseismological studies) carried out on the master fault of the Çaldıran fault zone by Güneyli et al. (2020), the slip rate and the return period of the peak earthquake to be sourced from the Çaldıran fault were determined once more as the 5.36 mm/yr and 280 yrs., respectively. Both the Deliçay and the Zilan Çayı, which amonate from the peak of the Aladağlar Mt. highland and then flow down-slope direction towards south, are cut and offset by the Çaldıran fault zone up to 12 km in dextral direction. Based on field observation, the slip rate on the Çaldıran fault zone is about 4.8 mm/yr. As is seen obviously from these descriptions, there is still no a common agrement about the slip rate along the Çaldıran fault zone.

5.4. Balıkgölü Fault Zone

This structure is an abaout 4-20 km wide, 127 km long (Turkish section) and NNW to NW trending active dextral strike-slip fault zone. It was first determined and reported by Arpat et al. (1977). It was also renamed and introduced to the international literature as the Gailatu (Balıkgölü)-Siah Cheshmeh-Khoy Fault (GSKF) comprising the northwestern section of the North Tebriz Fault System (Karakhanian et al., 2004; Mokhoori et al., 2021). Based on both the type and general trend, the Balıkgölü fault zone consists of two major sections: (1) Balıkgölü section and (2) the Arı Mountain section. The 35 km long and NNW trending Balıkgölü section consists of several parallel to sub-parallel, short normal fault segments cut and offset in left-lateral direction by NE trending sinistral strike-slip faults. The Quaternary Balıkgölü pull-apart basin lasts to develop on the down-thrown blocks of the normal fault segments (Figure 1b). The 92 km long and NW trending Arı Mountain section is situated between the southern coastal area of the Balıkgölü to the northwest and the Kızılkent-Gürbulak settlements to the southeast nearby the Turkish-Iranian State border (Figure 1b). This section consists of numerous fault segments of dissimilar size, trend and character. However, the NW trending dextral fault segments are prominent with respect to others. They bifurcate, rejoin and result in several lensoidal blocks with long axes more or less parallel to the general trend of the fault zone. Several pushups and pull-apart basins formed by the uplifting and subsidence of the lensoidal blocks, respectively. The more diagnostic of them is the Arı Mountain Pushup and the Doğubayazıt pull-apart basin (DPAB in Figure 1b). The Arı Mountain section is divided into two sub-sections around Doğubayazıt. The northern one passes across the state border and then continues as the Maku fault in NW Iran. However, the southern sub-section (the Kızılkent fault) psses the state border near by the Kızılkent Town and then runs in again SE direction in Iran. Lastly it joins with the Siah Cheshmeh-Khoy fault zone, which is the northwestern section of the North Tebriz Fault System (Figure 1b). Around the Turkish-Iranian State border, both the northerly situated Balıkgölü and the southerly located Çaldıran

fault zones are linked to each other by the intervening and N-S trending normal faults and related pull-apart basins such as the Uzunyol to Haramlı normal faults and the Çaldıran to Siyah Çeşme pull-apart basins. In addition, two of the most diagnostic extensional structures, namely the Tendürek Volcano and related geothermal field (DGF) of the late Quaternary age, also occur in the same area (Figure 1b). Numerous morphotectonic features, such as the triangular facets, steep to sub-vertical fault scarps, fault terraces, fault valleys, offset drainage systems, fault parallel-aligned to deformed alluvial fans and deltas, narrow-long to deep fault corridors, fault-parallel-aligned sag ponds to springs althogether, reveal that the Balıkgölü fault zone is active (Öztürk, 2020). In addition, based on both the field geological and GPS data the slip rate on the Balıkgölü fault zone is 2-3 mm /yr (Copley and Jackson, 2006).

5.5. Iğdır and Aras Fault Zones

This is an about 3-4 km wide, 75 km long and N60°W trending dextral strike-slip fault zone. It is located between Tuzluca County to the northwest and east of the Ağrı stratovolcano to the southeast (Figure 1b). The Iğdır fault zone determines and controls the southwestern margin of the Aras pull-apart basin. It is an approximately15-35 km wide, 200 km long and NW trending pull-apart basin situated among Türkiye, Armania and Nakhichevan (Azerbaijan). The Aras pull-apart basin is drained by the Aras drainage system and has a very thick (up to 250 m) Quaternary basin fill. The northern and the southwestern margins of this large depression are shaped by the Quaternary Alagöz (Aragast) and Ağrı strato volcanoes respectively. The Iğdır fault zone begins near the Tuzluca County to the northwest and then continues in southeastwards in several paralel to sub-paralel discontinues dextral strike-slip fault segments. The longest and continuous one is termed here as the Iğdır master fault. It cuts across the Cretaceous ophiolitic mélange (Kardeşli ophiolitic mélange), Quaternary volcanic rocks of Durak, Zor and Ağrı Mountains as well as the Quaternary basin fill, and then tectonically juxtaposes them with to each others (Figure 1b). A series of morphotectonic features, such as the fault-parallel aligned and deformed alluvial fans, hanging valleys, fault terraces, deflected to offset stream beds, triangular facets and steep fault scarps, indicate that the Iğdır master fault is geologically active. This was also proved once more by both the 6 July 1840 very destructive historical earthquake and the 4 September 1962 instrumental Iğdır earthquake of Mw = 5.6 sourced from the Iğdır master fault (Soysal et al., 1981; Karakhanian et al., 2002; 2004; Bozkuş et al., 2010). The 1840 Ağrı historical earthquake has also led to heavy damage, loss of numerous lifes in the surrounding settlements and large-scale mass-wasting events such as earth flows, floodings, rockfalls, debris flows, creep, liquefactions to lateral spreading of ground in a boroad area. In addition, the Ağrı volcano was reactivated once more and it started to pour out lavas and pyroclastites (Soysal et al., 1981; Karakhanian et al., 2002; 2004).

The Aras fault zone is 4-7 km wide, 120 km long and NW trending dextral strike-slip fault zone. It begins from the near north of rhe Artaşat City to the norhwest and then runs in southeastwards across the western Armenia and Nakhichevan countries. In the further southeast it joins with the Maku fault zone and then terminates. Its only the 54 km long Ararat section (central section) is included in the study area (Figure 1b). The Aras fault zone determines and controls the southestern margin of the Aras pull-apart basin. It consists of several fault segments, which cut both older rocks and Quaternary basin fill and tectonically juxtaposes them with to each others (Figure 1b). The bed of the Aras River is shifted towards the Aras fault zone along its whole length which implies to the activeness of the Aras fault zone.

Consequently, the whole of above-mentioned regional dextral active fault zones are linked to each other by the intervening extensional structures, such as the Aras, Siyah Çeşme, Çaldıran and Akpazar pull-apart basins and the N-S to NNW trending oblique-slip normal faults (Figure 1b). These regional strike-slip fault zones also display a northwestward-opening extensional horsetail structure characterized by both the DGF and the Ağrı to Tendürek volcanic cones of the the late Quaternary age which owe their origins to the same faulting mechanism.

6. Discussion on Geothermal Potential and Conceptual Model of East Anatolia

In general major factors, which control development of the geothermal fields, are active

tectonic regime and related faults, plate boundaries and/or proximity to them, shallow-seated Curie point depth (CPD), high heat flow, young volcanic activity, young hypabyssal intrusions with felsic to intermediate chemical compositions, thinned crust and ascended asthenospheric mantle, a thick package of rocks with high porosity or reservoir rock (s), a package of impermeable rocks or cover rocks, and meteoric water supply enough. These criteria were interpreted under the light of both the above-mentioned field geological data and the international literature, and a conceptual model for the geothermal potential of the eastern Anatolia were prepared (Figure 25).

As is seen in Figure 22, some regional dextral fault zones situated in the EATB, Armenia and Nakhichevan continue throughout the northwestern territory of Iran, approach to each others, and lastly join with the North Tebriz Fault system in the further southeast (Figure 22). Another to say, the North Tebriz Fault system bifurcates into several fault zones at its northwestern tip, and then results in an extensional horse tail structure (a releasing type of horse-tail splay faults structure) (Copley and Jackson, 2006; Masson et al., 2006; Djamour et al., 2011; Shabanian et al., 2012; Mokhoori et al., 2021). In addition, the northern half of this horse tail structure together with the Lesser Caucasus are moving towards northeast, i.e., this area is beeing expanded in NE-SW direction (large open arrows in Figure 22) (Jackson, 1992; Copley and Jackson, 2006; Reilinger et al., 2006), On the other hand, based on the geophysical studies carried out in eastern Anatolia, the average thickness of the crust ia 45 km (Zor et al., 2003), and there is no a mantle lithosphere beneath the continental crust, i.e., the continental crust is floating on the ascended and very hot (1285°C) asthenospheric mantle (Keskin, 2003; Barazangi et al., 2006). In this frame, the continental crust in eastern Anatolia is represented by the East Anatolian Accretionary Prism (Figures 24 and 25). Consequently, the origin of the Upper Miocene-Quaternary volcanism is a hybrit magma resulted from the partial melting along the crust-astenospheric mantle contact and contamination of the upwelling magma (Keskin, 2003; Açlan and Duruk, 2018). The total thickness of these volcanic rocks is about 2 km, and they represent the most significant cover rocks of the geothermal system in East Anatolia (Figure 25). In addition, the isolated Quaternary volcanic cones of mostly alkaline to calc-alkaline characters, such as the Ağırkaya, Meydan, Girekol, Etrüsk, Pirreşit, Kösedağ, Tendürek, Zor Mt., Durak Mt. and Ağrı volkanoes (Figure 24), represent the last phase of

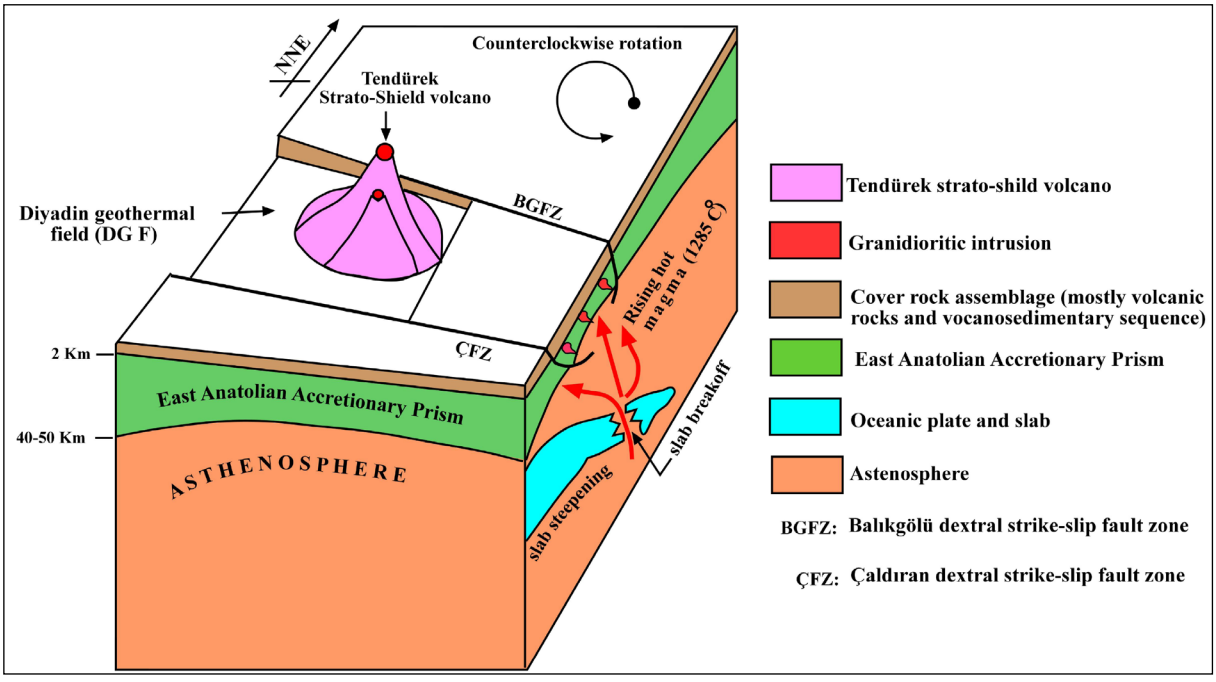

Figure 25- Sketched block diagram illustrating the geothermal heat source in eastern Türkiye.

the post-collisional magmatism in the east Anatolia. These isolated neotectonic volcanoes might have been underlain by a series of unroofed hypabyssal intrusions, which may also be the heat source of the geothermal fluid in the eastern Anatolia. For istance, the two-peaked Tendürek volcano is located near by the DGF. Its development lasted for about 0.7 Ma, and the last eruption on it took place 250.000 years ago, i.e., it is still active (Ölmez et al., 1994; Yılmaz et al., 1998; Lebedev et al., 2016). Another highest and neareast isolated volcano standing to the near northeast of DGF is the 5123 m high Ağrı stratovolcano. It was reactivated once more and poured out pyroclastites and lavas owing to the 1840 destructive historical Ağrı earthquake (Karakhanian et al., 2002). In particular, fumaroles along the foots of both volcanoes, numerous hot water springs to artesian wells and the actively forming fissure-ridge travertines in the DGF altogether reveal obviously that the geothermal potential of the DGF at the local scale, and the eastern Anatolia at regional scale are quite high (Basel et al., 2010; Pasvanoğlu, 2013; Şener and Şener, 2021). The temperature of the ascended asthenospheric mantle is about 1285°C (Figure 25). This value decreases in the opposite direction of geothermal gradient up to the 180°C at 1 km depth below the ground surface. Based on the studies carried out throughout the territory of Türkiye, the Curie temperature depth ranges between 14 and 18 km in the Ağrı region (Aydın et al., 2005; Akın et al., 2014, Elitok and Dolmaz, 2014). It is 16 km as an average. At this depth the Curie temperature is 585°C under normal conditions. In the same way, this value also decreases towards ground surface and becomes 210°C at one km depth below ground surface. In addition, the gases coming out of the Tendürek volcano is mantle in origin based on the isotope studies (Ölmez et al., 1994). Consequently, the source of the geothermal heat in eastern Türkiye is the ascended asthenospheric mantle (Keskin, 2003; Barazangi et al., 2006).

In general, the reservoir rocks in the East Anatolia are represented by the East Anatolian Accretionary Prism (EAAP). It was resulted from a series of tectono-sedimentary processes accompanied to the subduction and contint-continent collision between the northerly located Eurasian and southerly situated Arabian plate during the late Cretaceous-middle Miocene time. The EAAP is the tectono-sedimentary mixture of various rocks, such as the oceanic crust, deep-sea sedimentary sequence and the active to passive margins-drived older metamorphic rocks, in an ophiolitic materrial-rich finer-grained scaly matrix. It has been thrown into a series of imbricate stacks and overthickened at the time of obduction and tectonic transportation into its present-day position. The EAAP gained a considerable amount of permeability owing to the brittle deformation it experienced (Barazangi et al., 2006). The Kendel metamorphic rocks, made up of mostly marbles, are the blocks of dissimilar size floating rootless within the EAAP (Ölmez et al., 1994; Keskin, 2003; Lebedev et al., 2016). They are also very porus and full of caves owing to the easily dissolution of the $CaCO_3$. Thus, large-scale marble blocks also comprise another reservoir rock for the East Anatolian Geothermal System (Figure 25). The East Anatolia is also characterized by 2 km thick volcanic to volcanosedimentary rock sequence of dissimilar chemical compositions. In particularly pyroclastites, such as tuff and tuffite, are relatively finer-grained, and they result in secondary clay minerals owing to the chemical weathering processes. Thus they gain an impermeable texture. For this reason, the post-collisional volcanic to volcanosedimentary rocks comprise the cover rocks of the East Anatolian geothermal system (Figures 3, 7, 24 and 25).

The type locality, namely the DGF, is drained by the longest (722 km) drainage system, the Murat River, in the East Anatolia. It originates from the 3358 m high peak of the Aladağ Mt. in the further south and then flows downslow direction towards north and DGF (Figures 1b, 3 and 4a). The level of the water table around the upstream section (Aladağlar section) of the Murat River drainage system is about 20-25 m above the base level of the drainage system. However, it lowers up to 30 m and becomes 5-10 m below the base level in the further north around the DGF and the Akpazar pull-apart basin floor. Even though the precipitation in the type of snow and rain decreases in last 60 years, the elevation of the water table level is very close to the ground surface in the depressions. It is about 5 to 10 m below the ground surface in both the DGF and the Akpazar pull-apart basin. For istance, the elevation of the Akpazar pull-apart basin floor ranges from 1900 m to 1790 m, i.e., the water table elevation is between 1780 m and 1785 m. These observations reveal that the meteoric waters, which are necessary

for the development of the geothermal system in both the DGF and in the eastern Anatolia, are enough. These cold meteoric waters ara circulating deeper and deeper by using active faults and open fractures of active volcanoes untill they reach to the shallow-seated heeting source (e.g., most probably shallow-seated hypabyssal felsic to intermediate intrusions), and then turn back again towards ground surface as geothermal fluids by using the same kind of circulation paths.

The most of major Italian geothermal fields (IGF) are included in the Tyrrhenian back-arc region located on the western mountain front of the central Apennine orogeny chain (fold-thrust fault belt) (Batini et al., 2003; Giovanni et al., 2005). It is seen obviously that both the IGF and the DGF in eastern Türkiye have more or less same tectonic setting and ground surface manifestations, such as actively-growing to fossil fissure-ridge travertines, active volcanoes, fumeroles, numerous hot water springs to artesian wells, gas vents, widespread iron-rich alteration zones and active tectonic regimes and related faults, when they are compared (Giovanni, et al., 2005; Brogi and Capezzuoli, 2009; De Filippis et al., 2013, Porta et al., 2017). In contrary, there are also some significant contrasts between them. Among major contrasts, the followings can be mentioned: (1) the IGF has two basic reservoirs, which are the relatively shallow-seated (up to 2 km depth) sedimentary reservoir composed mostly of shallow-water platform to pelagic basin carbonates-turbidites of the late Triassic-Middle Miocene age and the deep-seated (up to 4 km depth) metamorphic basement rocks of Permian-early Triassic age (Giovanni et al., 2005; Santilano, 2016); whereas, the reservoir of the DGF is the accretionary prism of late Cretaceous age and the large-scale Upper Paleozoic-Mesozoic carbonate blocks to wedges in it experienced a multi-phased brittle deformation, (2) the cap rocks or the impermeable cover rocks of the IGF are represented by shallow-marine to terrestrial finer clastics of shale, marl, siltstone and volcanic tuff to tuffite intercalations of Plio-Quaternary age, whereas the DGF is characterized by a thick (up to 2 km) volcano-sedimentary sequence of Miocene-Quaternary age, (3) the geothermal fluids of the IGF are the superheated waters and gas (up to 350°-400°C) (Giovanni et al., 2005), whereas, the temperature of geothermal fluid of the DGF is relatively low (up to 150°C at the depth of 1 km), (4) the heat source of the IGF is relatively shallow-seated (up to depths of 3 and 6 km below ground surface) felsic to intermediate intrusions (Santilano, 2016), whereas the heat source of the DGF is still under debate.

7. Conclusions

Under the light of the above-mentioned dataset, the followins are concluded**:** (1) the strike-slip neotectonic regime in eastern Türkiye commenced at the time of latest Pliocene-early Quaternary time, and it triggerred the development of both the Tendürek strato-shild volcanoe and the Diyadin geothermal field, (2) the presence of main factors, which control the development of the geothermal system, was also determined in the eastern Türkiye; they obviously reveal that the geothermal potential of the eastern Türkiye is quite high as much as those in southwestern Anatolia. This is proved once more by its surface manifestations such as the active tectonic regime and related faults (e.g., extensional horsetail strucure), active volcanoes (Tendürek and Ağrı volcanoes), fumeroles, numerous hot water springs to artesian wells, widespread iron-rich alteration zones and actively growing thermogene fissure-ridge travertines. However, the heat source of the DGF is still under debate. For this reason, the probable presence of the unroofed hypabyssal felsic to intermediate intrusions at the roots and their near environs of the isolated Quaternary volcanoes in the eastern Türkiye have to be researched in detail by the geophysical methods.

Acknowledgements

This work has been financially supported by the Zorlu Energy Electricity Production Company, İstanbul. For this reason, authors of these paper are gratefull to the Zorlu Energy Company executives.

References

Açlan, M., Duruk, H. İ. 2018. Geochemistry, zircon U-Pb geochronology, and tectonic setting of the Taşlıçay Granitoids, Eastern Anatolia, Turkey. Arabian Journal of Geosciences 11 (36) 1-19.

Açlan, M., Turgut, İ. K. 2017. Şekerbulak (Diyadin-Ağrı) dolaylarında yüzeyleyen volkanik kayaçların mineralojik-petrografik ve jeokimyasal özellikleri. Çukurova Üniversitesi Mühendislik Mimarlık Fakültesi Dergisi 32 (4) 163-174.

Aghajany, S. H., Voosoghi, B., Yazdian, A. 2017. Estimation of north Tabriz fault parameters using neural networks and 3D tropospherically corrected surface displacement field. Geomatics, Natural Hazards and Risk 8 (2) 918-932.

Akın, U., Ulugergerli, E. U., Kutlu, S. 2014. Turkiye jeotermal potansiyelinin ısı akısı hesaplamasıyla değerlendirilmesi. Bulletin of the Mineral Research and Exploration 149, 205-214.

Aksoy, E., Tatar, Y. 1990. Van ili doğu-kuzeydoğu yöresinin stratigrafisi ve tektonigi. TÜBITAK Doğa Dergisi 14**,** 628-644.

Aksoy, E., İnceoz, M., Koçyiğit, A. 2007. Lake Hazar basin: a negative fl ower structure on the East Anatolian fault system (EAFS), SE Turkiye. Turkish Journal of Earth Sciences 16, 319–338.

Altunel, E. 1996. Pamukkale travertenlerinin morfolojik özellikleri, yaşları ve neotektonik önemleri. Bulletin of the Mineral Research and Exploration 118, 47-64.

Altunel, E., Hancock. P. L. 1993. Active fissuring and faulting in Quaternary travertines at Pamukkale, western Turkey. Geomorphology 94, 285-302.

Altunel, E., Karabacak, V. 2005. Determination of horizontal extension from fissure-ridge travertines: a case study from the Denizli Basin, southwestern Turkey. Geodinamica Acta 18, 333-342.

Ambraseys, N. N., Jackson, J. A. 1998. Faulting associated with historical and recent earthquakes in the Eastern Mediterranean region. Geophysical Journal International 133, 390-406.

Arpat, E., Şaroğlu, F., Iz, H. B., 1977. Çaldıran depremi. Yeryuvarı ve İnsan 2, 29-41.

Atabey, E. 2002. The formation of fissure ridge type laminated travertine-tufa deposits microscopical cheacteristics and diagenesis, Kirşehir, central Anatolia. Bulletin of the Mineral Research and Exploration 123-124,59-65.

Avagyan, A., Sosson, M., Philip, H., Karakhanian, A., Rolland, Y., Melkonyan, R., Rebai, S., Davtyan, V. 2005. Neogene to Quaternary stress field evolution in Lesser Caucasus and adjacent regions using fault kinematics analysis and volcanic cluster data. Geodinamica Acta 18 (6) 401-416.

Aydın, H., Karakuş, H., Mutlu, H. 2020. Hydrogeochemistry of geothermal waters in eastern Turkey: Geochemical and isotopic constraints on water-rock interaction. Journal of Volcanology and Geothermal Research 390, 106708.

Aydın, İ., Karat, H. İ., Koçak, A. 2005. Curie point depths map of Turkey. GJI Volcanology, geothermics fluids and rocks 162, 633-640.

Barazangi, M., Sandvol, E., Seber, D. 2006. Structure and Tectonic Evolution of the Anatolian Plateau in Eastern Turkey. Geological Society of America, Special Paper 409, 463–473.

Basel, E. D. K., Serpen, U., Satman, A. 2010. Turkey's geothermal Energy potential: updated results. Proceedings, Thirthy-Fifth Workshop on Geothermal Reservoir Engineering. Stanford University, Stanford, California, February 1-3.

Batini, F., Brogi, A., Lazzarotto, A., Liotta, D., Pandeli, E. 2003. Geological features of Larderello-Travale and Mt. Amiata geothermal areas (Southern Tuscany, Italy). Episodes 26(3), 239-244.

Bozkuş, C., Demir, M., Kurtuluş, B. 2010. Iğdır ve yakın çevresinin depremselliği. ReaserchGate, 15.

Brogi, A., Capezzuoli, B. 2009. Travertine deposition and faulting: the fault-related travertine fissure-ridge at Terme S. Giovanni, Rapolano Terme (Italy). International Journal of Earth Sciences 98, 931-947.

Brogi, A., Capezzuoli, A., Costantini, A., Gandin, A., Lazzarotto, A. 2005. Tectonics and travertines relationship in the Rapolano Terme area (Northern Apennines, Italy). Proceedings of the First International Symposium on Travertine, 142-148.

Brogi, A., Capezzuoli, E., Karabacak, V., Alçiçek, M.C., Luo, L. 2021. Fissure Ridges: A Reappraisal of Faulting and Travertine Deposition (Travitonics). Geosciences 2021, 11, 278.

Canbaz, C. H., Temizel, C., Palabiyik, Y., Balıkçıoğlu, A., Yılmaz, I. Ö., Aytuna, S., Ranjith, R. 2020**.** Evaluation of Geothermal Potential of Turkey as an Alternative Source of Energy Under Demand and Supply Dynamics of Other Energy Resources. Conference paper. Turkey IV. Scientific and Technical Petroleum Congress, 20 December 2020 in Turkey.

Copley, A., Jackson, J. 2006. Active tectonics of the Turkish-Iranian Plateau. Tectonics 25, 1–19.

Çolak, S., Aksoy, E., Kocyiğit, A., Inceoz, M. 2012. Palu-Uluova strike-slip basin on the East Anatolian Fault System, Turkey: transition from paleotectonic period to neotectonic period. Turkish Journal of Earth Sciences 21 (4), 547-570.

De Filippis, L., Anzalone, E., Billi, A., Faccenna, C., Poncia, P. P., Sella, P. 2013. The origin

and growth of a recently-active fissure ridge travertine over a seismic fault, Tivoli, Italy. Geomorphology 195,13–26.

Demirel, V., Ozkan, H. 2000. Ağri-Diyadin MT-2, 3 and 4 Geothermal Well Drilling, Completion Report. Maden Tetkik ve Arama Genel Müdürlüğü Report No. 10451, 1-14 (in Turkish).

Demir, S. 2006. Hydrogeological investigation and Detection of the Origin of Thermal Waters in Diyadin. Istanbul Technical Univ. MSc Thesis (in Turkish).

Demirkıran, Z., Elçi, H. 2022. Urganlı (Manisa) Travertenlerinin Morfolojik Özellikleri ve Tektonizma ile İlişkisi. Mühendislik Bilimleri ve Tasarım Dergisi 10(3), 1027-1042.

Dewey, J. F., Hempton, M. R., Kidd, W. S. F., Şaroğlu, F., Şengör, A. M. C. 1986. Shortening of continental lithosphere: the neotectonics of eastern Anatolia-a young collision zone. Collision Tectonics. Geological Society of London Special Publication 19, 3-36.

Doğan, U., Koçyiğit, A., Yılmaz, E. 2019. Geomorphological evolutionary history of the Melendiz River Valley, Cappadocia, Turkey .Mediterranean Geoscience Reviews 1, 203-222.

Dhont, D., Chorowicz, J. 2006. Review of the neotectonics of the Eastern Turkish-Armenian Plateau by geomorphic analysis of digital elevation model imagery. International Journal of Earth Sciences 95, 34-49.

Djamour, Y., Andrnant, P., Nankali, H. R., Tavakoli, F. 2011. NW Iran-eastern Turkey present-day kinematics: Results from the Iranian permanent GPS network. Earth and Planetary Science Letters 307, 27–34.

Elitok, Ö., Dolmaz, M. N. 2014. Mantle flow-induced crustal thinning in the area between the easternmost part of the Anatolian plate and the Arabian Foreland (E Turkey) deduced from the geological and geophysical data. Gondwana Research 13, 302-318.

Emre, Ö., Duman, T. Y., Elmacı, H., Olgun, Ş., Özalp, S. 2012. 1/250.000 ölçekli Türkiye Diri Fay Haritası Serisi, Doğubayazıt (NJ 38-2) nolu pafta seri No. 54, Maden Tetkik ve Arama Genel Müdürlüğü, Ankara, Türkiye.

Emre, Ö., Duman, T. Y., Özalp, S., Şaroğlu, F., Olgun, Ş., Elmacı, H., Çan, T. 2018. Active fault databese of Turkey. Bulletin of Earthquake Engineering 16(8), 3229-3275.

Ercan, T., Fujitani, T., Madsuda, J., Nodsu, K., Tokel, S., Tadahide, U. I. 1990. Doğu ve Güney-doğu Anadolu Neojen-Kuvaterner volkanitlerine ilişkin yeni jeokimyasal, radyometrik ve izotopik verilerin yorumu. Bulletin of the Mineral Research and Exploration 110, 143-164.

Ercan, T., Keskin, İ., Dönmez, M. 1993. Eleşkirt (Ağrı) Yöresindeki Tersiyer Yaşlı Volkanizmanın Jeokimyasal Özellikleri ve Bölgesel Yayılımı. Jeoloji Mühendisleri Dergisi 42, 74-88.

Ercan, T., Sümengen, M. 2018. Türkiye Jeoloji Haritaları Serisi, Doğubayazıt Paftası, No. 254. Maden Tetkik ve Arama Genel Müdürlüğü, Jeoloji Etütleri Dairesi, Ankara (unpublished), Türkiye.

Esirtgen, T., Hepsen, N. 2018. Türkiye Jeoloji Haritaları Serisi, Doğubayazıt J51 Paftası, No. 256. Maden Tetkik ve Arama Genel Müdürlüğü, Jeoloji Etütleri Dairesi, Ankara, Türkiye.

Giovanni, B., Guido, C., Adolfo, F. 2005. Characteristics of Geothermal Fields in Italy. Giornale di Geologia Applicata 1, 247 -254.

Güneyli, H., Yaman, M., Yıldırım, V. 2020. Çaldıran Fayı'nın Çaldıran İlçesi Dolayında Paleosismolojik ve Neotektonik Özellikler. Çukurova Üniversitesi Mühendislik Mimarlık Fakültesi Dergisi 35(2), 279-293.

Hancock, P. L., Chalmers, R. M. L., Altunel, E., Çakır, Z. 1999. Travitonics: using travertines in active fault studies. Journal of Structural Geology 21, 903-916.

Hempton, M. R. 1987. Constraints on Arabian plate motion and extensional history of the Red Sea. Tectonics 6, 687-705.

Hessami, K., Pantosti, D., Tabassi, H., Shabanian, E., Abbassi, M. R., Feghhi, K., Solaymani, S. 2003. Paleoearthquakes and slip rates of the North Tabriz Fault, NW Iran: Preliminary results. Annales de Geophysique, 46, 903-916.

Innocenti, F., Mazzuoli, R., Pasquare, G., Radicati, F., Villan, L. 1976. Evolution of the volcanism in the area of interaction between the Arabian, Anatolian, and Iranian plates (Lake Van., Eastern Turkey). Journal of Volcanology and Geothermal Research 1,103-112.

Innocenti, F., Mazzuoli, R., Päsquare, G., Scrri, G., Villari, L. 1980. Geology of the volcanic area north of Lake Van (Turkey). Geologische Rundschau 69(1), 292-323.

Jackson, J. 1992. Partitioning of strike-slip and convergent motion between Eurasia and Arabia in eastern Turkey and the Caucasus. Journal of Geophysical Research: Solid Earth 97, 12471-12479.

Kalender, L., Öztekin, Ö., İnceöz, M., Çetindağı. B., Yıldırım, V. 2015. Geochemistry of travertine deposits in the Eastern Anatolia District: an example of the Karakoçan-Yoğunağaç (Elazığ) and Mazgirt-Dedebağ (Tunceli) travertines, Turkey. Turkish Journal of Earth Sciences 24, 1-20.

Kansun, G., Afzali, A. O., Üçgün, F. 2020. The Stratigraphic and Petrographic Properties of the Rocks in Davut -Tazekent Vicinity, Diyadin-Ağrı-Turkey. European Journal of Science and Technology Special Issue 528-551.

Karabacak, V. 2007. Ihlara vadisi (Orta Anadolu) travertenlerinin genel ozellikleri ve kabuksal deformasyon açısından onemleri. Eskişehir Osmangazi Universitesi Muhendislik Mimarlık Fakultesi Dergisi 20, 65-82 (in Turkish).

Karabacak, V., Mutlu, H. 2019. Sarıhıdır Travertenlerinin (Avanos) jeokronolojik ve İzotopik Sistemleri: Acıgöl ve Erciyes Volkanizmasına Ait Geç Kuvaterner Kabuk deformas-yonu tarihlendirilmesi. Maden Tetkik ve Arama Genel Müdürlüğü Project Number:118Y069, 96.

Karakhanian, A., Djrbashian, R., Trifonov, V., Philip, H., Arakelian, S., Avagian, A. 2002. Holocene-historical volcanism and active faults as natural risk factor for Armenia and adjacent countries. Journal of Volcanology and Geothermal Research 113 (1– 2), 319-344.

Karakhanian, A. S., Trifonov, V. G., Philip, H., Avagyan, A., Hessami, K. 2004. Active faulting and natural hazards in Armenia, eastern Turkey and northwestern Iran. Tectonophysics 380,189-219.

Keskin, M. 2003. Magma generation by slab steepening and slab-breakoff beneath a subduction accretion complex: an alternative model for collision-related volcanism in eastern Anatolia, Turkey. Geophysical Research Letters 30, 8046–8050.

King, G. C. P., Nabelek, J. L. 1985. Role of Fault Bends in the Initiation and Termination of Earthquake Rupture. Science 228, 983-987.

Kıral, K., Çağlayan, A. 1980. Kağızman (Kars)-Taşlıçay (Ağrı) dolayının Jeolojisi. Maden Tetkik ve Arama Genel Müdürlüğü, Jeooji Etütleri Dairesi, Report Number: 154 (unpublished).

Koçyiğit, A. 2005. Denzili Graben-Horst System and the eastern limit of the West Anatolian continental extension: basin fill, structure, deformational mode, throw amount and episodic evolutionary history, SW Turkey. Geodinamica Acta 18, 167-208.

Koçyiğit, A. 2008. Orta Anadolu'nun Aktif tektoniği ve jeotermal enerji potansiyeli. Middle East Technical University, Faculty of Science, Deaprtment of Geological Engineering Project Number: 07-03-091-00-23, Final Report, 135.

Koçyiğit, A. 2013. New field and seismic data about the intraplate strike-slip deformation in Van region, East Anatolian plateau, E. Turkey. Journal of Asian Earth Sciences 62, 586-605.

Koçyiğit, A. 2022. Diyadin (Ağrı) ilçe sınırları içinde yer alan 30 Nolu Gedik Köyü ve 31 Nolu Mutlu Köyü Ruhsat sahalarının jeotermal potansiyeli ile ilgili saha jeolojisi çalışmaları: Technical Report, 75 (unpublished).

Kocyiğit, A., Beyhan, A. 1998. A new intracontinental transcurrent structure: the Central Anatolian Fault Zone, Turkey. Tectonophysics 284, 317–336.

Koçyiğit, A., Canoğlu, C. 2017. Neotectonics and seismicity of the Erzurum pull-apart basin, East Turkey. Russian Geology and Geophysics 58, 99-122.

Koçyiğit, A., Doğan, U. 2016. Strike-slip neotectonic regime and related structures in the Cappadocia region: a case study in the Salanda basin, Central Anatolia, Turkey. Turkish Journal of Earth Sciences 25, 393–417.

Koçyiğit, A. Yılmaz, A., Adamia, S., Kuloshvili, S. 2001. Neotectonics of East Anatolian Plateau (Turkey) and Lesser Caucasus: implication for transition from thrusting to strike-slip faulting. Geodinamica Acta 14, 177-195.

KOERI 2022. Akçift (Muradiye-Van) earthquake. Boğaziçi Üniversitesi, Kandilli Rasat-hanesi ve Deprem Araştırma Enstitüsü, İstanbul.

Lebedev, V. A, Sharkov, E. V., Ünal, E., Keskin, M. 2016. Late Pleistocene Tendürek Volcano (Eastern Anatolia, Turkey):I. Geochronology and Petrographic Characteristics of Igneous Rocks. Petrology 24(2), 127-152.

Mancini, M., Marini, M., Moscatelli, M., Pagliaroli, A., Stigliano, F., Di Salvo, C., Simionato, M., Cavinato, G. P., Corazza, A. 2014. A physical stratigraphy model for seismic microzonation of the Central Archaeological Area of Rome (Italy). Bulletin of Earthquake Engineering 12, 1339 – 1363.

Masson, F., Djamour, Y., Van Gorp, S., Chery, J., Tatar, M., Tavakoli, F., Nankali, H., Vernet, P. 2006. Extension in NW Iran driven by the motion of the South Caspian Basin. Earth and Planetary Science Letters 252, 180-188.

Mesci, B. L., Erkmen, A. C., Gürsoy, H., Tatar, O. 2018. Fossil findings from the Sıcak Çermik fissure ridgetype travertines and possible hominid tracks, Sivas, Central Turkey. Geodinamica Acta 30(1), 15-30.

Mesci, B. L., Gürsoy, H., Ghaleb, B., Tatar, O. 2020. An Extensional Fracture Acting as Hot Water Source for Travertine Deposition on the North Anatolian Fault Zone, Turkey: the Reşadiye Fissure-Ridge. Geological Bulletin of Turkey 63, 145-1607.

Mesci, B. L., Gürsoy, H., Tatar, O. 2008. The evolution of travertine masses in the Sivas area (Central Turkey) and their relationships to active tectonics. Turkish Journal of Earth Sciences 17, 219-240.

Mokhoori, A. N., Rahimi, B., Moayyed, M. 2021. Active tectonic stress field analysis in NW Iran-NE Turkey using earthquake focal mechanism data. Turkish Journal of Earth Sciences 30, 235-246.

MTA 2018. General Directorate of Mineral Research and Exploration, Energy Maps.

MTA 2021. Turkey Geothermal Resources Distribution and Application Map.

Mutlu, H., Aydın, H., Kazancı, A. 2013. Diyadin (Ağrı) jeotermal sahasına yönelik jeokimyasal ve izotopik bulgular. 11. Ulusal Tesisat Mühendisleri Kongresi, İzmir, 47-67.

Ölmez, E., Ercan, T., Yıldırım, T. 1994. Tendürek (Doğu Anadolu) Jeotermal Alanının (Diyadin, Zilan, Çaldıran) Volkanolojisi ve Jeotermal Enerji Olanakları, 47. Türkiye Jeoloji Kurultayı Bildiriler Kitabı, 49-55.

Özgür, N., Kıymaz, I., Uzun, E., Kutlu, D. S. 2017. Hydrogeological modelling of geothermal waters in Pamukkale, western Anatolia, Turkey. European Geologist 43, 52-58.

Özkul, M., Varol, B., Alçiçek C. 2002. Deposıtıonal Envıronments and Petrography of Denizli travertınes. Bulletin of the Mineral Research and Exploration 125, 13-29.

Öztürk, Y. 2020. Aktif fayların tanımlanmasında jeomorfik belirteçlerin rolü: Balıkgölü fay zonu örneği. Jeomorfolojik Araştırmalar Dergisi 5, 101-117.

Porta, G. D., Croci, A., Marini, M., Kele, S. 2017. Deposıtıonal Architecture, Facies Character and Geochemical Sıgnature of the Tıvoli Travertines (Pleistocene, Acque Albule Basin, Central Italy). Rivista Italiana di Paleontologia e Stratigrafia (Research in Paleontology and Stratigraphy) 123(3), 487-540.

Pasvanoğlu, S. 2013. Hydrogeochemistry of thermal and mineralized waters in the Diyadin (Ağrı) area, Eastern Turkey. Applied Geochemistry 38, 70-81.

Pearce, J. A., Bender, J. F., de Long, S. E., Kidd, W. S. F., Low, F. J., Güner, Y., Şaroğlu, F., Yılmaz, Y., Moofbath, S., Mitchell, J. G. 1990. Genesis of collision volcanism in Eastern Anatolia, Turkey. Journal of Volcanology and Geothermal Research 44,189-229.

Reilinger, R., McClusky, S., Vernant, P., Lawrence, S., Ergintav, S., Cakmak, R., Ozener, H., Kadirov, F., Guliev, I., Stepanyan, R., Nadariya, M., Hahubia, G., Mahmoud, S., Sakr, K., ArRajehi, A., Paradissis, D., Al-Aydrus, A., Prilepin, M., Guseva, T., Evren, E., Dmitrotsa, A., Filikov, V., Gomez, F., Al-Ghazzi, R., Karam, G. 2006. GPS constraints on continental deformation in the Africa-Arabia-Eurasia continental collision zone and implications for the dynamics of plate interactions. Journal of Geophysical Research 111, B05411.

Sağlam-Selçuk, A., Kul, A. Ö. 2021. Long-term slip rate estimation for Ercis Fault in East Anatolian Compressive Tectonic Block from geologic and geomorphologic field evidence. Geological journal 56, 5290-5310.

Sağlam-Selçuk, A., Erturaç, M. K., Nomade, S. 2016. Geology of the Çaldıran Fault, Eastern Turkey: Age, slip rate and implications on the characteristic slip behavior. Tectonophysics, 680, 155-173.

Sağlam-Selçuk, A., Erturaç, M. K., Uner, S., Özsayınç, E., Pons-Branchud, E. 2017. Evolution of Çamlık fissure-ridge travertines in the Başkale basin (Van, Eastern Anatolia) Geodinamica Acta 29(1), 1-19.

Santilano, A. 2016. Deep geothermal exploration by means of electromagnetic methods: New insights from the Larderello geothermal field (Italy). PhD. thesis in the Graduate School of Politecnico di Torino, 242.

Serpen, U., Aksoy, N., Ongurc, T., Korkmaz, E. D. 2009. Geothermal energy in Turkey: 2008 update. Geothermics 38, 227-237.

Shabanian, E., Acocella, V., Gioncada, A., Ghasemi, H., Belieri, O. 2012. Structural control on volcanism

in intraplate post collisional settings: Late Cenozoic to Quaternary examples of Iran and Eastern Turkey. Tectonics 31, TC3013.

Sharkov, E., Lebedev, V., Chugaev, A., Zabarinskaya, L., Rodnikov, A., Sergeeva, N., Safonova, I. 2014. The Caucasian-Arabian segment of the Alpine-Himalayan collisional belt: geology, volcanism and neotectonics. Geoscience Frontiers 6, 513-522.

Soysal, H., Sipahioğlu, S., Kolçak, D., Altınok, Y. 1981. Türkiye ve Çevresinin Tarihsel Deprem Kataloğu (2100 B.C.–1900 A.D.). TÜBİTAK, TBAG-341.

Sümengen, M. 2009. 1/100.000 ölçekli Türkiye Jeoloji Haritaları Serisi, Kars H50 Paftası. Maden Tetkik ve Arama Genel Müdürlüğü, Report Number:108, Ankara, Türkiye.

Şaroğlu, F., Yılmaz, Y. 1986. Doğu Anadolu›da neotektonik dönemdeki jeolojik evrim and havza modelleri Bulletin of the Mineral Research and Exploration 107,73-94.

Şaroğlu, F., Emre, Ö., Boray, A. 1987. Türkiyenin Diri Fayları ve Depremselliği. Maden Tetkik ve Arama Genel Müdürlüğü, Report Number: 8174 Ankara (unpublished).

Şener, M. F. 2018. Akhüyük (Konya) Jeotermal Alanındaki Hidrotermal Akışkan Dolaşımı ve Traverten Oluşum Mekanizması, Orta Anadolu, Türkiye. Türkiye Jeoloji Bülteni 61, 193-206.

Şener, E., Şener, Ş. 2021. Exploration of geothermal potential using integrated fuzzy logic and analytic hierarchy process (AHP) in Ağrı, Eastern Turkey. Turkish Journal of Earth Sciences 30,1134-1150.

Şengör, C., Kidd, W. S. F. 1979. Post-collisional tectonics of the Turkish-Iranian plateau and a comparison with Tibet. Tectonophysics 55, 361-376.

Şengör, C., Yilmaz, Y. 1981. Tethyan evolution of Turkey A plate tectonic approach. Tectonophysics 75, 181-241.

Tan, O., Tapırdamaz, M. C., Yörük, A. 2008. The Earthquake Catalogues for Turkey. Turkish Journal of Earth Sciences 17, 405-418.

Temiz, U., Savas, F. 2018. U/Th Dating of the Akhuyuk fissure ridge travertines in Ereğli, Konya (Central Anatolia, Turkey): their relationship to active tectonics. Arabian Journal of Science and Engineering 43,3739-3749.

Temiz, U., Gokten, E., Eikenberg, J. 2009. U/Th dating of fissure ridge travertines from the Kırşehir region (Central Anatolia Turkey). Structural relations and implications for the Neotectonic development of the Anatolian block. Geodinamica Acta 22, 201-213.

Temiz, H., Koçak, İ., Öksüz, N., Akbay, S. 2021. Significance of neotectonic and paleoclimatic Late Pleistocene-Holocene travertine and origins: Balkayası, Avanos-Nevsehir, Central Anatolia/ Turkey. International Journal of Earth Sciences 110(6), 2157-2177.

Toksöz, M. N., Arpat, E., Şaroğlu, F. 1977. East Anatolian Earthquake of 24 November 1976. Nature 270, 423-425.

Türkecan, A., Dönmez, M., Özgür, T. B., Mutlu, G., Sevin, D., Bulut, V. 1992. Patnos-Tutak-Hamur (Ağın) yöresinin jeolojisi ve volkanik kayaçların petrolojisi. Maden Tetkik ve Arama Genel Müdürlüğü Report Number: 9434 Ankara (unpublished).

Üçgün, F. 2019. The Petrography-Geochemistry of Volcanic Rocks Around in Davut- Tazekent Villages (Diyadin-Ağrı) and the Characteristics of the Diyadin Geothermal Field, MSc, Selcuk University, Konya, Turkey (in Turkish).

Üçgün, F., Kurt, M., Karagöz, K., Kocaman, S., Zilbeyaz,, N., Göçer, H., Erol, F., Tanışır, E., Çeker, S. 2014. Ağrı İli Minerallı Sular Araştırması. T.C. Serhat Kalkınma Ajansı Ağrı Destek Ofisi, Proje Sonuç Raporu, 164.

Van Noten, K., Soete, J., Claes, H., Foubert, A., Özkul, M., Swennen, R. 2013. "Fracture networks and strike-slip deformation along reactivated normal faults in Quaternary travertine deposits, Denizli Basin, Western Turkey". Tectonophysics 588, 154-170.

Vignaroli, G., Mancini, M., Brilli, M., Bucci, F., Cardinali, M., Giustini, F., Voltaggio, M., Yu, T. L., Shen, C. C. 2020. Spatial-Temporal Evolution of Extensional Faulting and Fluid Circulation in the Amatrice Basin (Central Apennines, Italy) During the Pleistocene. Frontiers in Earth Science 8, 130.

Yeşilova, Ç. 2021. Potential geoheritage assessment; Dereiçi travertines, Başkale, Van (east anatolian Turkey). MANAS Journal of Engineering 9(1), 66-71.

Yıldırım, G. 2018. Akkaya-Eskipazar (Karabük) travertenine yönelik jeokimyasal ve izotopik bulgular. Ankara Üniversitesi Jeoloji Mühendisliği Bölümü, Yüksek Lisans Tezi, 87.

Yılmaz, Y., Güner, Y., Şaroğlu, F. 1998. Geology of the Quaternary volcanic centers of the east Anatolia. Journal of Volcanology and Geothermal Research, 85, 173-210.

Yılmaz, Y., Şaroğlı, R., Güner, Y. 1987. Initation of the neomagmatism in East Anatolia. Tectonophysics 134, 177-199.

Zor, E., Sandvol, E., Gürbüz, C., Türkelli, N., Seber, D., Barazangi, M. 2003. The crustal structure of the East Anatolian plateau (Turkey) from Receiver functions. Geophysical Research Letters 30 (24), 8044.